

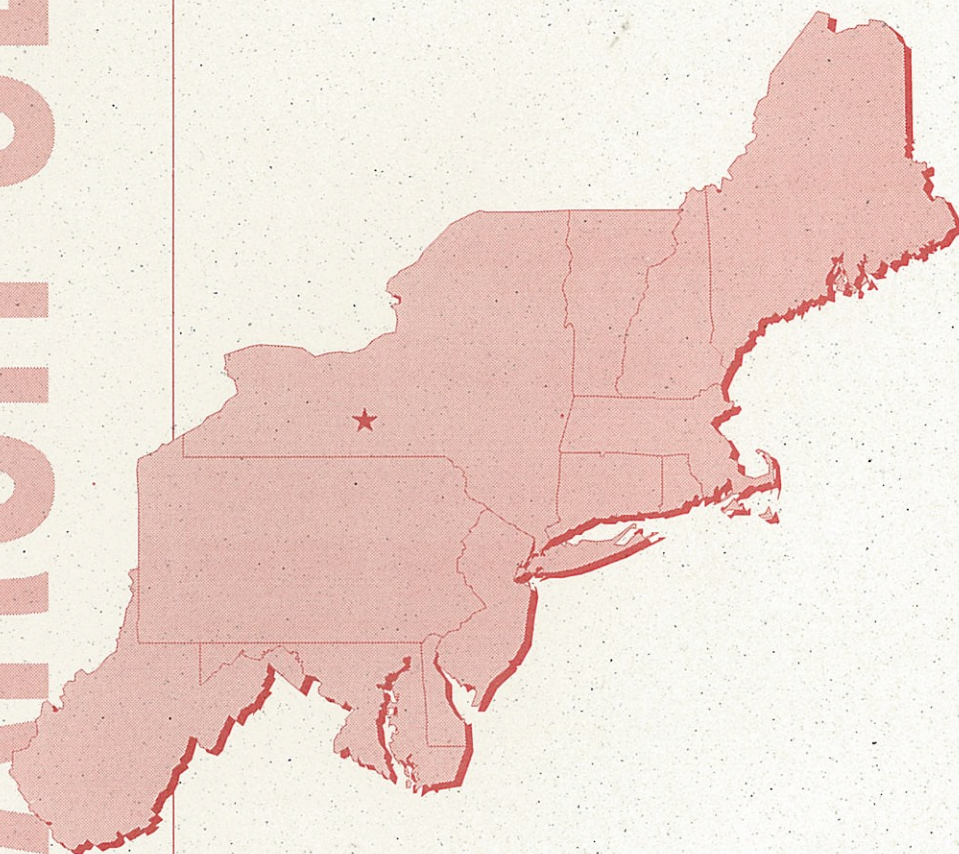
NORTHEAST REGIONAL CLIMATE CENTER

Atlas of Soil Freezing Depth Extremes for the Northeastern United States

Arthur T. DeGaetano

Daniel S. Wilks

Megan McKay



**Cornell University
Ithaca, New York**

Publication No. RR 96-1
March 1996

The mission of the Northeast Regional Climate Center (NRCC) is to facilitate and enhance the collection, dissemination and use of climate data as well as to monitor and assess climatic conditions and impacts in the twelve-state, northeastern region of the United States. Implementing this mission involves three programmatic objectives: 1) the development and management of regional climate data bases, 2) the dissemination of information and educational services regarding climate and its impacts, and 3) the performance and support of applied climate research.

Established in 1983, the Northeast Regional Climate Center (NRCC) is one of six regional climate centers now operating throughout the nation. These regional centers serve as sources of climate data and information to public and private institutions and individuals as well as expertise on local and regional climate problems. The Center's staff cooperate with State Climatologists and research scientists in disseminating climate data and information, analyzing environmental and economic impacts of climate variability, and developing new applications of weather and climate data for agriculture, business, industry, and government operations.

The NRCC Research Report series is intended to make available to interested users the full results of climate research that has been supported by the NRCC. This report series supplements the normal reporting of research results in professional journals and provides an outlet for more complete and comprehensive accounts of work performed than is generally possible in journals.

For further information please write or call:

Northeast Regional Climate Center

1123 Bradfield Hall
Cornell University
Ithaca, New York 14853-1901
(607) 255-1751



The Northeast Regional Climate Center is supported by a Grant from the National Oceanic and Atmospheric Administration.

Atlas of Soil Freezing Depth Extremes for the Northeastern United States

Arthur T. DeGaetano

Daniel S. Wilks

Megan McKay

Northeast Regional Climate Center

Research Series

Publication No. RR 96-1

March 1996

CONTENTS

I. Explanatory Material

Introduction	1
Description of Model	1
a. Technical Details	1
b. Verification	3
Computation of Return Periods	4
a. Data	4
b. Extreme-value Analysis	5
Return Period Mapping	6
a. Explanation of Return Periods	6
b. Gridding, Interpolation and Contouring	7
Sensitivity to Soil Characteristics	8
Acknowledgment	9
References	9
Station List	12

II. Climatic Maps

Maximum Depth Under Bare Soil

Map 1. 2-year return period	15
Map 2. 5-year return period	16
Map 3. 10-year return period	17
Map 4. 25-year return period	18
Map 5. 50-year return period	19
Map 6. 100-year return period	20

Maximum Depth Under Sod

Map 7. 2-year return period	21
Map 8. 5-year return period	22
Map 9. 10-year return period	23
Map 10. 25-year return period	24
Map 11. 50-year return period	25
Map 12. 100-year return period	26

Maximum Depth Under Snow-free Bare Soil

Map 13. 2-year return period	27
Map 14. 5-year return period	28
Map 15. 10-year return period	29
Map 16. 25-year return period	30
Map 17. 50-year return period	31
Map 18. 100-year return period	32

INTRODUCTION

Extreme values of the maximum depth of soil freezing are of interest for engineering design specifications. For instance, building codes must consider the maximum depth of frost penetration to assure that footings and utilities are buried at the appropriate depths. If these specifications are too lax, freezing conditions are likely to result in structural damage during the design lifetime of the structure. Alternatively, codes that are too stringent inflate building costs unnecessarily due to increases in labor and material costs. Unfortunately, the only direct practical analysis of maximum soil freezing depths in the U.S. is based on unofficial, undocumented and antiquated (1899-1938) measurements (USDA 1941). More recently, Crandell et al. (1994) present a map of 100-year return period air freezing indices which can be used to derive empirical frost depth values. However, these values neglect the effects of a changing winter snow cover.

This paucity of measured frost depth data has led us to develop a one-dimensional heat flow model capable of estimating frost depths using only meteorological variables measured at cooperative network weather stations (DeGaetano et al., 1996a). Given that approximately 900 cooperative network stations are in the Northeast, model-derived frost depths can be developed for a relatively dense network of sites across this region. Using these modeled frost depth estimates, an extreme-value climatology for the maximum depth of soil freezing is produced.

This atlas presents extreme annual maximum soil freezing depth statistics in the form of average return periods for the 12-state region designated as the northeastern United States for purposes of the Regional Climate Center program of the National Weather Service, National Oceanic and Atmospheric Administration. These states are Connecticut, Delaware, Maine, Maryland, Massachusetts, New Hampshire, New Jersey, New York, Pennsylvania, Rhode Island, Vermont, and West Virginia. Data from the states of Ohio, Kentucky and Virginia have also been included in this project to complete the representation of the mapped fields within the map rectangle encompassing the northeastern U.S. The Canadian portion of the map rectangle is blank because the requisite climatological snow depth data are unavailable.

DESCRIPTION OF MODEL

a. Technical Details

Although DeGaetano et al. (1996a) give a full description of the model used to derive this climatology, a brief outline of the model is included in this section to acquaint users with the method used to calculate daily soil freezing estimates. The theoretical basis for the model is that the process of frost penetration is driven

primarily by thermal diffusion. Figure 1 illustrates this principle. At the lower boundary, Z_D , which is set at a depth of 2 m (or greater if soil freezing extends past this depth), a daily “deep” temperature T_D is given as a function of the average air temperature over a period from the previous April through March of the current year, the 25th percentile January through March snow depth for the current year and the combined thermal diffusivity of the snow and soil. The model assumes that the flux of heat through the lower boundary is negligible.

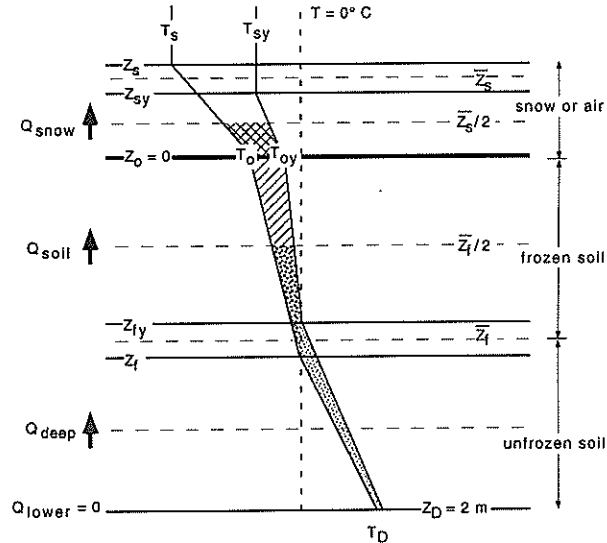


Figure 1. Schematic diagram showing the model's frozen soil state. Depths below or above (in the case of snow and/or air) the surface are indicated by Z and temperatures are indicated by T . Subscripts indicate snow (s), frozen soil (f), the soil surface (0), and the lower boundary (D). The subscript “ y ” refers to the value observed or estimated for the previous day. Heat fluxes through the centers of each layer are indicated by the bold arrows. The stippled area represents the change in energy storage ΔQ_l and the hatched areas represent ΔQ_f .

The upper boundary condition is given by the observed average daily air temperature. Here the assumption is made that the average daily air temperature is representative of the temperature of the snow surface. The snow depth (Z_s) gives the thickness of the first layer in the snow/soil system (Fig. 1). In the absence of snowcover, the air temperature is assumed to equal the temperature at the upper surface of a 1.0×10^{-3} m laminar layer, the thermal properties of which are characteristic of still air. Progressing downward, soil layers of variable depth are defined by frozen and unfrozen zones, the boundaries of which are at 0°C (Fig. 1). A maximum of three soil layers (one frozen and two unfrozen) is allowed by the model.

Temperature gradients through each layer are assumed to be linear, and thus the heat fluxes at the middle of each layer, Q_x , are defined by the differences between the temperatures of the layer boundaries. Imbalances between the resulting vertical heat fluxes (i.e. heat flux convergence or divergence) are rectified through internal temperature changes and, when these changes cross 0°C , freezing or thawing of an appropriate depth of soil. In this process, the fluxes are balanced by accounting for the heat capacities of soil solids and soil water, and for the latent heat of fusion. This is sketched in Figure 1 and given mathematically for the case when a frozen layer exists at the surface by the governing equation

$$Q_{snow} = Q_{froz} = Q_{deep}, \quad (1)$$

where

$$Q_{snow} = -K_{snow}(T_s - T_0)/Z_s + \Delta Q_U, \quad (2)$$

$$Q_{froz} = K_{froz}(T_0/Z_f) + \Delta Q_L, \quad (3)$$

and

$$Q_{deep} = K_{thaw}T_D/(Z_f - Z_D) + (Z_{fy} - Z_f)(\epsilon - 0.1)L_f. \quad (4)$$

The variables used in Equations 1-4 are defined in Figure 1 with the exception of the latent heat of freezing (L_f), soil porosity (ϵ), thermal conductivities of snow (K_{snow}), frozen soil (K_{froz}), and unfrozen soil (K_{deep}) and the change in heat storage terms (ΔQ). Equations 1-4 are solved numerically for the prognostic variables T_0 and Z_f . Nearly-saturated soil moisture conditions are assumed at all times. In Figure 1, ΔQ_U is represented by the (upper) hatched and cross-hatched areas between the two consecutive daily average temperature profiles. Similarly, ΔQ_L is shown by the (lower) speckled and dotted regions.

Only one of three possible soil-freezing states is illustrated by Figure 1. In this state a layer of frozen soil extends from the surface to some depth, Z_f . The other possible states are that the soil may remain unfrozen from the surface to the lower boundary, Z_D , or a layer of frozen soil may exist between two layers of unfrozen soil. In addition, five transition modes are possible, corresponding to the transitions between the three basic states with the exception of the transition from unfrozen to a buried frozen layer, which is not physically realizable.

The model is initiated in the unfrozen state and continues in this manner until T_0 falls below 0°C . At this point, the transition to frozen soil mode is activated. Provided the temperature remains below 0°C on subsequent days, the model operates in the frozen soil mode. In this state, both soil freezing and thawing occur at the bottom of the frozen layer. When T_0 exceeds 0°C the model transitions to either the unfrozen or surface thaw state. In the surface thaw state, the layer of frozen soil is allowed to thaw both from its top and bottom. The temperature throughout the buried frozen layer which results is assumed to be a constant 0°C . For subsequent occurrences of $T_0 < 0^\circ\text{C}$ freezing occurs at the both the top and bottom of the buried frozen layer. Although physically unrealistic, in that freezing should be allowed to occur at the top of the surface-thaw layer, this formulation allows a solution without liberal assumptions regarding the temperature profile within a subsurface thawed layer. Given that the purpose of our model is to estimate the depth of maximum frost penetration, the omission of a second frozen layer at the surface is of little consequence.

b. Verification

Validation of the model was possible using frost depth data collected with six Army Corps of Engineers frost depth tubes (Ricard et al., 1976). These gauges were installed at the Ithaca, New York cooperative observer network site, allowing coincident soil-freezing and daily meteorological data to be collected. Three gauges were placed under sod. The remaining gauges were located within a bare soil plot. Frost depth measurements were made on a weekly basis. Verification trials for the winter of 1995-1996 using these data are presented in Figure 2. A more rigorous model validation appears in DeGaetano et al (1996a).

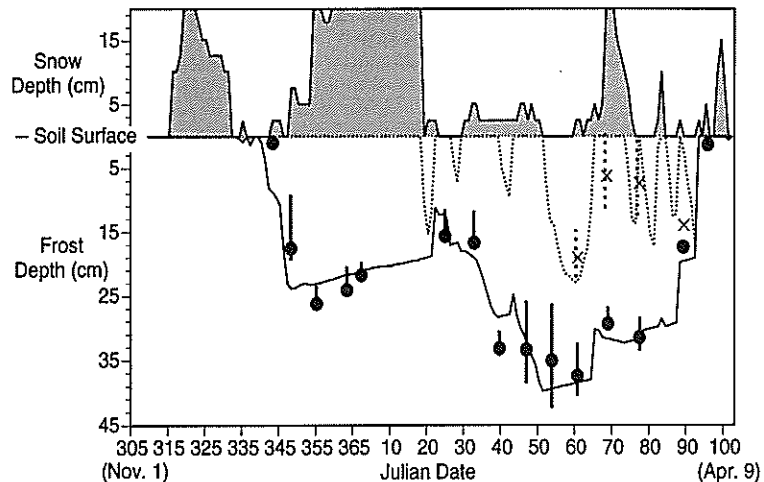


Figure 2. Observed versus estimated frost depths under a bare soil surface at Ithaca, NY for the winter of 1995-96. Modeled frost depths and surface thaw depths are given by the solid and dashed lines, respectively, shown below the soil surface. The bars show the range of three frost depth observations, with bold dots identifying the median. Dashed vertical lines and Xs similarly indicate observed thawing. Only two frost depth measurements were available on Julian days 38, 59, 66, 75 and 87. Daily snow depths are indicated by the gray regions above the surface.

During the winter of 1995-96, observed maximum frost depths under bare soil ranged from 42 to 26 cm, with a median frost depth of 34 cm measured by the third gauge (Fig. 2). In all cases, the maximum frost depth occurred on 21 February. During this winter, the maximum model-derived value of 40 cm occurred on 20 February indicating exceptional correspondence between the observations and model estimate in both the timing and magnitude of maximum soil freezing. Over the course of the winter the model tracks the timing and progression of soil freezing quite closely (Fig. 2). Over the 15 soil freezing observations shown in Figure 2, the model exhibits a 1.8 cm bias toward overestimation of the observed frost depth, with a mean absolute error of 3.4 cm. Similar validation accuracy was obtained for the shallower freezing under sod-covered surfaces.

COMPUTATION OF RETURN PERIODS

a. Data

Annual model-derived maximum frost depths were calculated for a set of 306 northeastern U.S. cooperative network stations (Fig. 3 and Table 1). To be included, stations were required to have at least 30 years of non-missing daily climatological data. At all sites serially complete daily temperature data (DeGaetano et al., 1995) was available for one of four periods (1951-1993; 1951-1990, 1961-1993 or 1961-1990). Serially complete snow depth and precipitation data were not available. If missing, these parameters were estimated using data from adjacent stations, or in the case of snow depth, based on previous and subsequent daily observations. Years were not considered if any missing data values occurred for more than 7 consecutive days during October through April. During the remaining months, the corresponding 30-year daily temperature normal was used as an estimate for missing temperature and any missing precipitation-based variables were set to zero. A more rigorous estimation

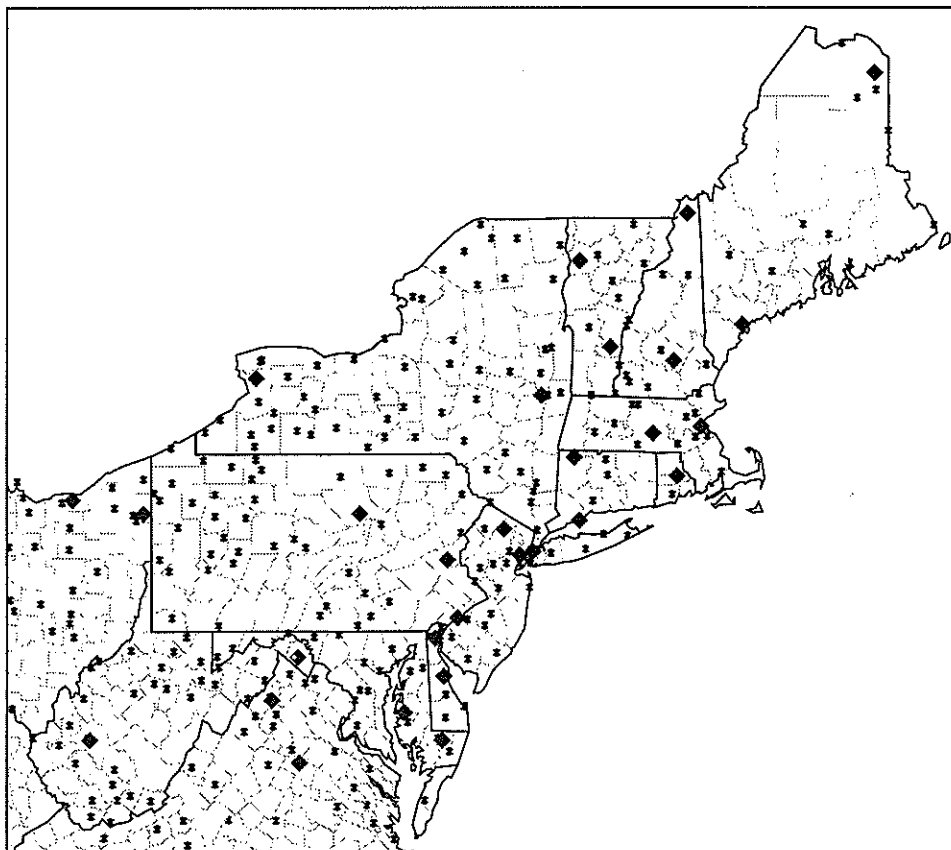


Figure 3. Locations of stations used to develop the extreme soil freezing climatology. At least 30 annual maximum frost depth values are available at each site. Diamonds indicate those stations used to develop adjustment factors in Figure 4 for varying soil characteristics.

scheme was not required during these months since data were only required for specification of the “deep” temperature wave. In all cases, the meteorological data were required to pass the quality-control procedure of Robinson (1993)

b. Extreme-value Analysis

Since the data records for all of the stations used in this atlas range from 30 to 43 years, soil freezing depth estimates for the 50- and 100-year return periods have been extrapolated beyond the observed data. These extrapolations have been achieved by fitting a theoretical probability function to the observed annual frost depth maxima at each station. Soil freezing depths corresponding to shorter (i.e. not necessarily extrapolated) return periods have also been computed using the fitted probability functions, in order to smooth sampling irregularities. In all cases, the modelled annual extremes have been represented using the Gumbel distribution (Wilks, 1995), which was found in exploratory work to give the best results among eleven candidate distributions for extreme soil freezing data in the northeastern U.S. (DeGaetano et al., 1996b). The probability density function for this distribution is

$$f(x) = \frac{1}{\beta} \exp \left\{ -\exp \left[-\frac{(x - \xi)}{\beta} \right] - \frac{(x - \xi)}{\beta} \right\}, \quad (5)$$

where x is the random variable (in this case, annual maximum frost depths). The distribution has two parameters: ξ is a location parameter, and β is a scale parameter. Separate distributions are fit to the data for each station by maximum likelihood, using the Levenberg-Marquardt method (Press et al., 1986). One convenient feature of the Gumbel distribution is that it is analytically integrable, so that its cumulative distribution function can be written in closed form. That is, Gumbel probabilities can be obtained using

$$F(x) = \Pr\{X \leq x\} = \int_0^x f(x)dx = \exp\left\{-\exp\left[-\frac{(x-\xi)}{\beta}\right]\right\}. \quad (6)$$

Average return periods, R , relate to cumulative probabilities, F , of the distributions of annual maximum data according to

$$R = \frac{1}{\omega[1 - F(x)]}, \quad (7)$$

where ω is the average sampling frequency, in this case 1 yr^{-1} . Subsequently, frost depths, x , corresponding to specified return intervals are obtained by solving Equation 6 for x and substituting the expression $F(x) = 1 - 1/R$, obtained by rearrangement of Equation 7. These operations yield the expression for frost depths as a function of return period and the parameters of the fitted Gumbel distribution,

$$x = \xi - \beta \ln[-\ln(1 - \frac{1}{R})]. \quad (8)$$

RETURN PERIOD MAPPING

Three sets of soil freezing extreme maps depicting the spatial distributions of maximum frost depths for specific return intervals are presented in this atlas. Maps 1-6 show the 2-, 5-, 10-, 25-, 50- and 100-year return periods for the maximum annual depth of soil freezing under bare soil. Similarly, Maps 7-12 show soil freezing extremes under sod-covered surfaces. Maps 13-18 depict soil freezing extremes under snow-free bare soil.

Although the stations represented in Maps 1-18 represent the densest spatial resolution available for the region, data-sparse areas are apparent, most notably across most of Maine. Users should exercise caution in extrapolating the mapped soil freezing depths to these areas. Similarly, Cember and Wilks (1993) noted that the cooperative observer network underrepresents local mean elevations in the Northeast by as much as 150 m. These differences are most pronounced along the northern Appalachians from western Massachusetts to western Maine, and over the Adirondack and Catskill Mountains in New York. In these areas, however, it is likely that the bias toward warmer temperatures introduced by the lower-elevation cooperative observer network is offset to a large extent by the presence of a deeper and more persistent snowcover at higher elevations. These opposing biases should act to minimize elevation-dependent influences on the mapped soil freezing fields.

a. Explanation of Return Periods

The annual extreme soil freezing depth isopleths (contour lines) drawn in Maps 1-18 correspond to "average return periods". That is, it is estimated that soil freezing depths as deep or deeper than the magnitudes shown on the maps will be separated,

on average, by the number of years given by the return period. It is important to realize that the actual times between two soil freezing episodes of a particular magnitude are not expected to correspond exactly to the return period. Rather, over the course of centuries, the average of the separation times between pairs of these episodes should be close to the specified return period. Thus, the soil freezing depth corresponding to the 100-year return period, might not occur in a given century, but could occur more than once in some other century. In a hypothetical average over many centuries, however, one would expect about as many occurrences of the 100-year soil freezing depth at a given location as the number of centuries being averaged.

b. Gridding, Interpolation and Contouring

Maps 1-18 were prepared by transferring the maximum frost depths from each individual station to an array of grid points, and then producing contour maps from the grid point values by automated means. Frost depths were transformed into a 54×82 (latitude \times longitude) grid, with points spaced at 0.2° intervals. Stations outside of the rectangle defined by this grid were also used to improve the placement of contours near the edges of the grid. The gridding algorithm used finds the smallest circle around each gridpoint that encloses at least two stations, where the circle radius is an integer multiple of 0.2 great-circle degrees. If the circle has a radius of 1.4° or less, the grid point is assigned a weighted average of the enclosed station values.

Each grid point value is computed as

$$x_g(\lambda_g, \phi_g) = \frac{\sum_{i=1}^I w_i(\lambda_g, \phi_g, \lambda_i, \phi_i) x_i(\lambda_i, \phi_i)}{\sum_{i=1}^I w_i(\lambda_g, \phi_g, \lambda_i, \phi_i)}, \quad (9)$$

where w_i is a modified McLain (1974) weighting function

$$w_i(\lambda_g, \phi_g, \lambda_i, \phi_i) = \frac{\sqrt{N_i} \exp \left[-\frac{\cos^2 \phi_0 (\lambda_g - \lambda_i)^2 + (\phi_g - \phi_i)^2}{d_{scale}^2} \right]}{f + \frac{\cos^2 \phi_0 (\lambda_g - \lambda_i)^2 + (\phi_g - \phi_i)^2}{d_{scale}^2}} \quad (10)$$

In Equations 9 and 10, x represents frost depth, λ is longitude, ϕ is latitude, the subscript g refers to the grid point, the subscript i distinguishes among the I individual cooperative network stations within each circle, and N_i is the sample size (number of winters of record) of the modeled maximum frost depth data at station i . The parameter d_{scale} is a scaling distance, $\phi_0 = 42.45^\circ$ is a reference latitude and $f=10^{-6}$ is a small constant to prevent division by zero.

The gridded fields are smoothed using the moving average in a 3×3 cell window (i.e. by an unweighted average of each grid point with its eight adjacent neighbors). These smoothed gridded values were then contoured and plotted using the NCAR Graphics Software package, version 3.2 (Clare and Kennison, 1989).

SENSITIVITY TO SOIL CHARACTERISTICS

The frost depths shown in Maps 1-18 depict results for soils having a clay content of 15% and a porosity of 45%. Non-clay soil particles are assumed to be quartz-based. It is further assumed that air occupies 10% of the available soil volume and that any remaining pore space is filled with water. Although this limits the model's application to wet soil conditions, this restriction is of little consequence over regions such as the northeastern United States, where high levels of soil moisture are typical during the period of soil freezing. In order to quantify the effect of differing clay contents and porosities on modeled annual maximum frost depths, a geographically representative set of 30 stations was selected. These sites are shown by diamonds in Figure 3. At each of these sites separate frost depths corresponding to the 2-, 5-, 10-, 25-, 50- and 100-year return interval were calculated using soil porosities ranging from 30 to 60% in increments of 5%. Similarly frost depths were computed for clay contents of ranging from 2 to 50%, holding porosity constant at 45%. Separate sensitivity analyses were conducted for bare soil, sod and snow-free bare soil.

Modification of the the clay content had little effect on the depth of soil freezing. In general, the difference in maximum soil freezing depth between the standard (15% clay content) and either clay content extreme (2 or 50%) was less than 5%. Changes in porosity, and thus water content, had a more pronounced effect on the maximum depth of frost penetration. Figure 4 shows these differences in maximum frost penetration as a ratio (multiplied by 100) of the annual maximum freezing depth based on the given porosity to that which occurred using the 45% standard porosity. Since the station-to-station and return period-to-return period differences in the ratios was quite small (generally ≤ 0.03) the values shown in Figure 4 are the medians over the 30 stations and 6 return periods.

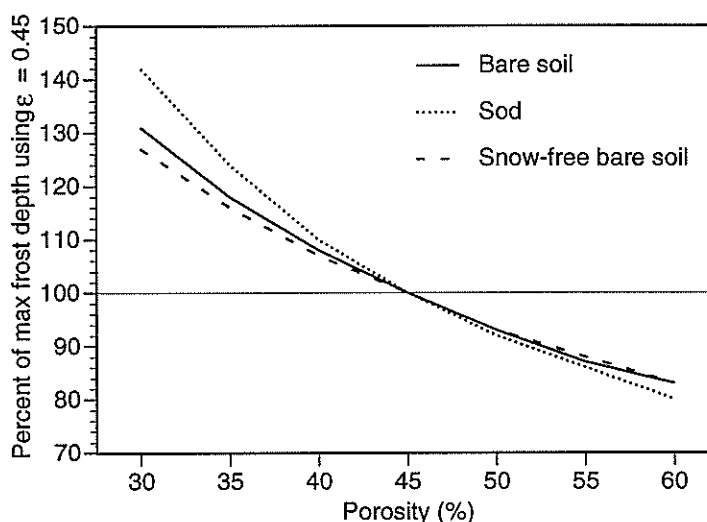


Figure 4. Graph of adjustment factors (percent of the maximum frost depth using a standard soil porosity of 0.45) used to convert the maximum frost depth values presented in Maps 1-18 to values representative of a site-specific soil porosity. Adjustment factors are medians over the 30 stations and 6 return periods.

With the exception of the two lowest porosities, the ratios shown in Figure 4 are generally insensitive to surface cover type. In general, maximum frost depths increase by as much as 45% for porosities below the standard. Alternatively, the larger

porosities are associated with shallower soil freezing. In application, Figure 4 can be used to adjust the maximum frost depth values presented in Maps 1-18 to values representative of a site-specific soil porosity. For example, to compute a 100 year return period frost depth for a bare-soil site in New York City having a soil porosity of 55%, the 60 cm value given presented in Map 6 is multiplied by 0.89 yielding a depth of 53 cm.

ACKNOWLEDGMENT

The encouragement of Jay Crandell of the National Association of Homebuilders Research Center was greatly appreciated. This work was supported by NOAA Grant NA16CP-0220-01.

REFERENCES

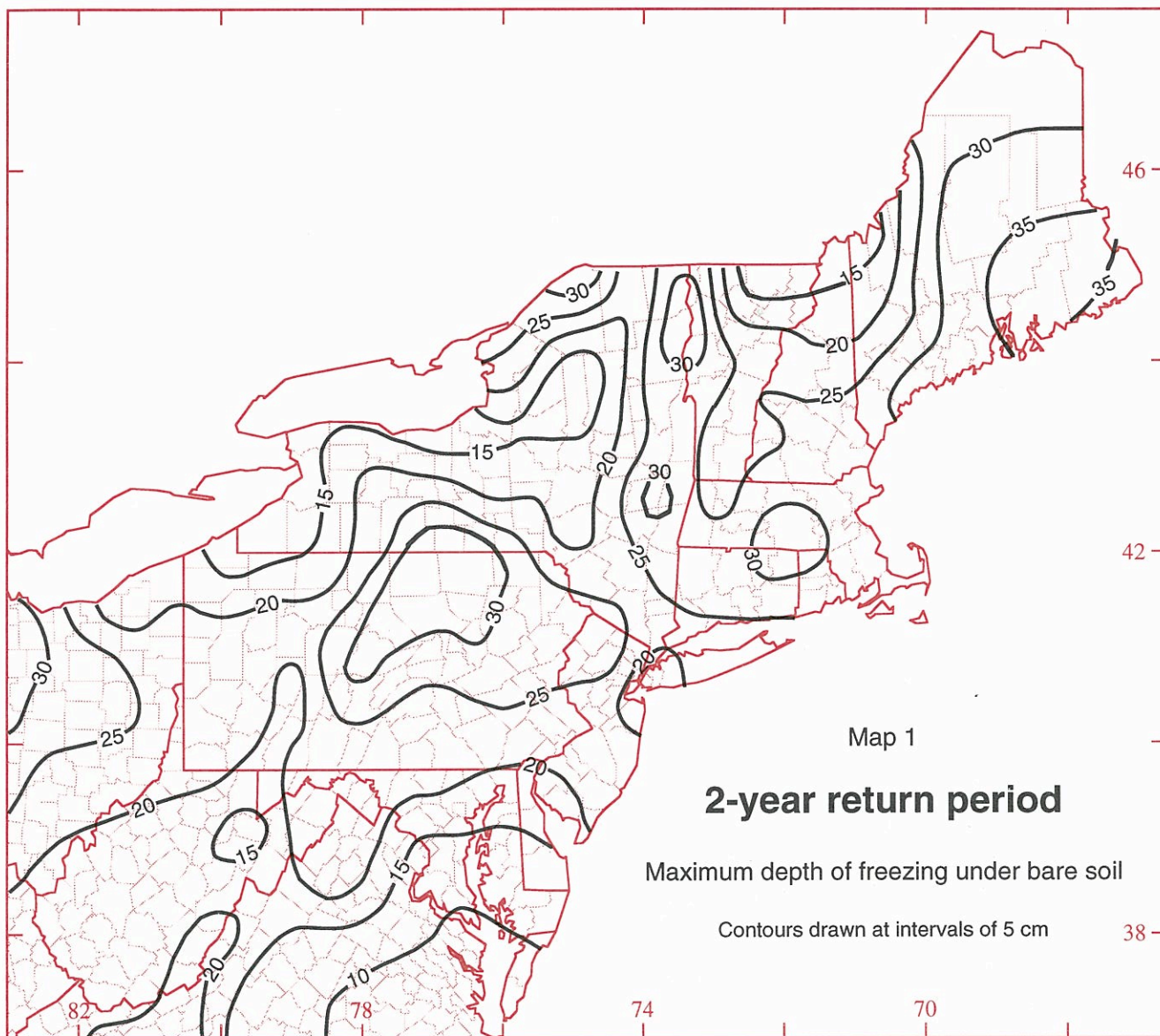
- Cember, R.P., and D.S. Wilks, 1993: *Climatological atlas of snowfall and snow depth for the northeastern United States and southeastern Canada*. Publication RR 93-1, Northeast Regional Climate Center, Cornell Univ., Ithaca, NY, 216 pp.
- Clare, F., and D. Kennison, 1989: *NCAR Graphics Guide to New Utilities*, National Center for Atmospheric Research, Boulder, Colorado, 439 pp.
- Crandell, J.H., E.M. Lund, M.G. Bruen, and M.S. Nowak, 1994: *Design guide for frost-protected shallow foundations*. Report available from the National Homebuilders Association Research Center, 400 Prince George's Blvd., Upper Marlboro, MD 20772.
- DeGaetano, A.T., K.L. Eggleston, and W.W. Knapp, 1995: A method to estimate missing daily maximum and minimum temperature observations. *J. Appl. Meteor.*, 34, 371-380.
- DeGaetano, A.T., D.S. Wilks, and M. McKay, 1996a: A physically-based model of soil freezing in humid climates using air temperature and snow cover data. *J. Appl. Meteor.*, 35, 1009-1027.
- DeGaetano, A.T., D.S. Wilks, and M. McKay, 1996b: Extreme-Value Statistics for Frost Penetration Depths in the Northeastern U.S., *Journal of Geotechnical and Geoenvironmental Engineering*, [accepted].
- McLain, D.H., 1974: Drawing contours from arbitrary data points. *Computer Journal*, 17, 318-324.
- Press, W.H., S.A. Teukolsky, W.T., Vetterling, and B.P. Flannery, 1992: *Numerical Recipes in FORTRAN The Art of Scientific Computing 2nd Ed.* Cambridge University Press, New York, N.Y., 963 pp.
- Ricard, J.A., W. Tobiasson, and A. Greatorrex, 1976: *The Field Assembled Frost Gage*. U.S. Army Corps of Engineers Cold Regions Research and Engineering Laboratory Technical Note, 7 pp.
- Robinson, D.A., 1993: Historical daily climatic data for the United States. Preprints American Meteorological Society Eighth Conference on Applied Climatology, Anaheim, CA, 264-269.

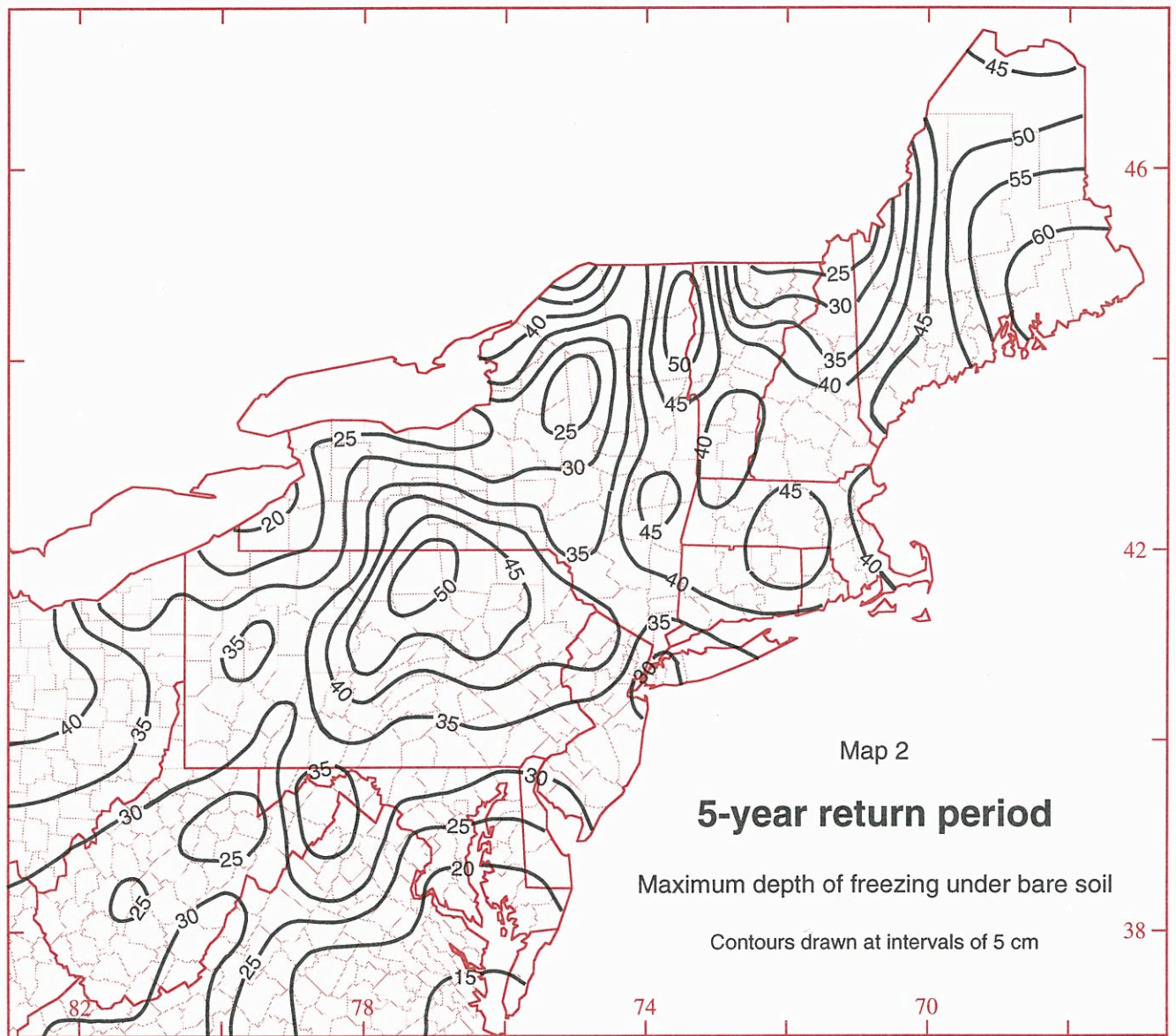
- USDA, 1941: *Climate and Man, Yearbook of Agriculture 1941*. U.S. Government Printing Office, Washington, DC, 1248 pp.
- Wilks, D.S., 1995: *Statistical Methods in the Atmospheric Sciences*. Academic Press, San Diego, CA, 464 pp.

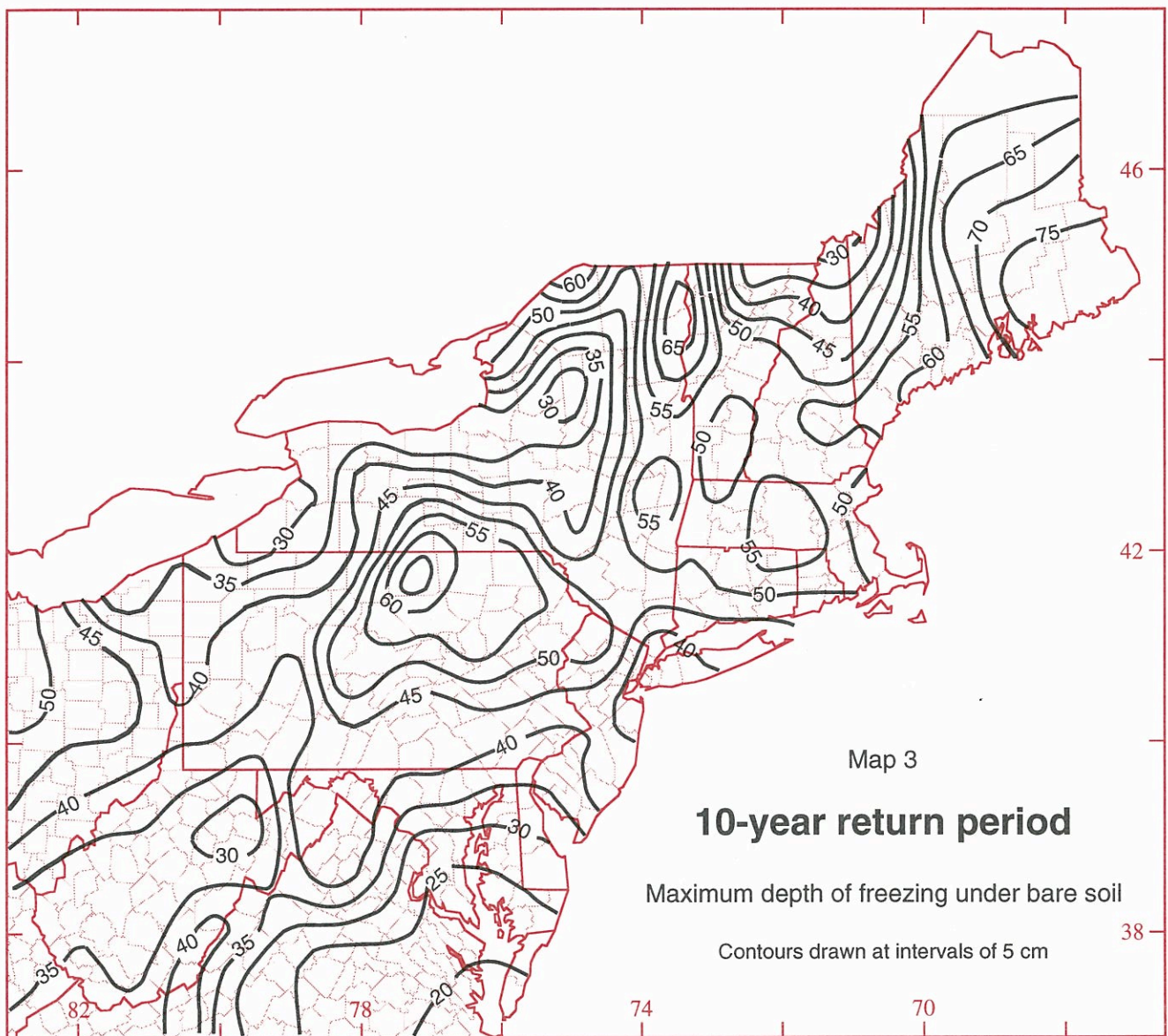
Table 1. List of stations used and their locations.

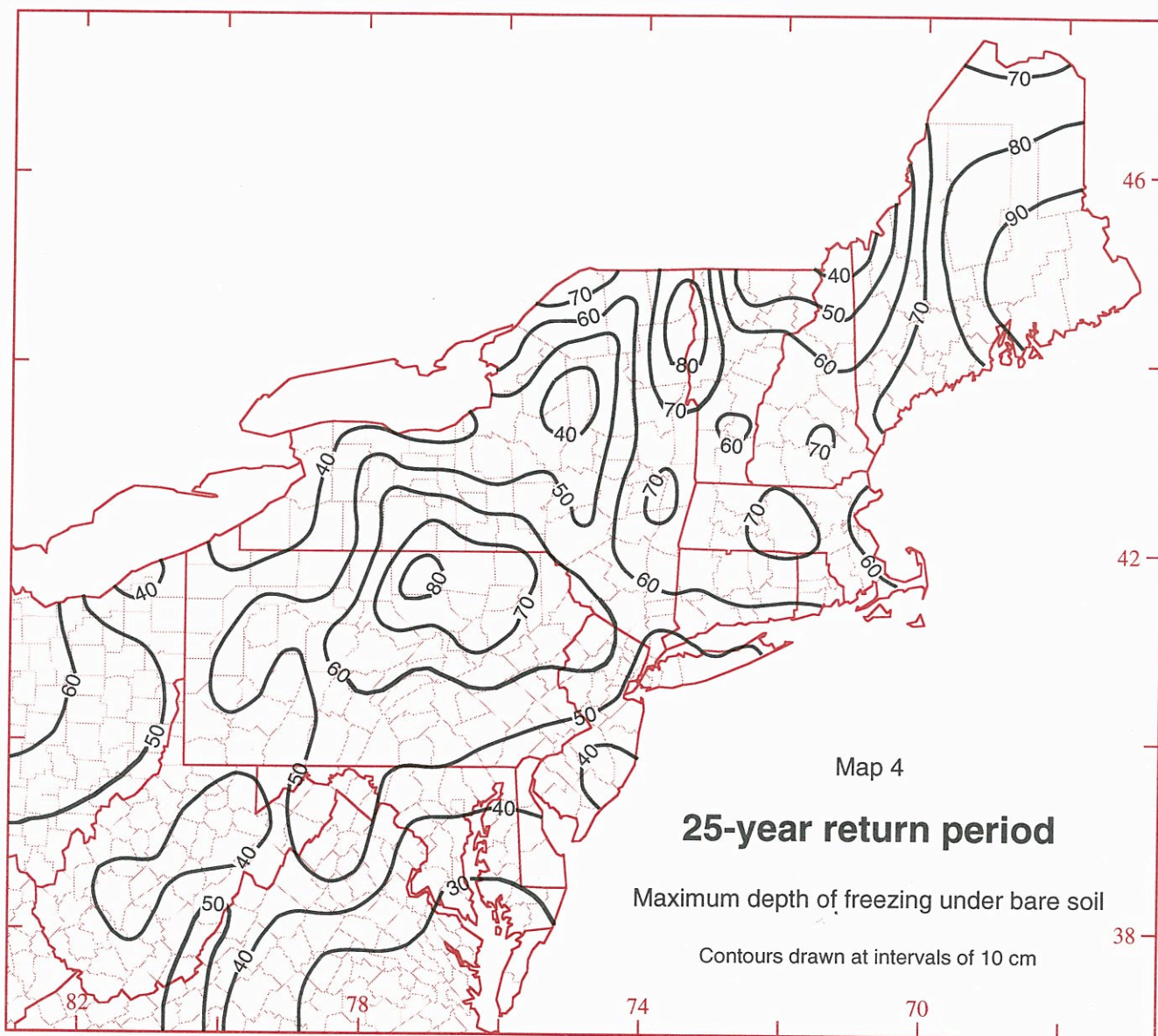
Station #	Station name	Latitude (degrees)	Longitude (degrees)	Station #	Station name	Latitude (degrees)	Longitude (degrees)
CONNECTICUT				NEW JERSEY (continued)			
060806	BRIDGEPORT WSO AP	41.17	73.13	286177	NEWTON	41.04	74.78
063451	HARTFORD BRAINARD FIELD	41.73	72.65	286843	PEMBERTON 1 E	39.95	74.67
063456	HARTFORD WSO AIRPORT	41.93	72.68	287079	PLAINFIELD	40.60	74.40
065077	MOUNT CARMEL	41.40	72.90	288194	SOMERVILLE	40.59	74.63
065445	NORFOLK 2 SW	41.97	73.22	289910	WOODSTOWN 2 NW	39.65	75.35
DELAWARE				NEW YORK			
072730	DOVER	39.15	75.52	300042	ALBANY WSFO AP	42.75	73.80
073570	GEORGETOWN 5 SW	38.63	75.46	300085	ALFRED	42.25	77.78
075320	LEWES	38.77	75.13	300093	ALLEGANY STATE PARK	42.10	78.75
075915	MILFORD	38.92	75.45	300183	ANGELICA	42.30	78.02
076410	NEWARK UNIVERSITY FARM	39.66	75.75	300220	ARCADE	42.53	78.42
079595	WILMINGTON WSO ARPT	39.67	75.60	300331	AURORA RESEARCH FARM	42.73	76.65
079605	WILMINGTON PORTER RSVR	39.77	75.53	300443	BATAVIA	42.99	78.18
KENTUCKY				300448	BATH	42.34	77.34
152791	FARMERS	38.14	83.55	300687	BINGHAMTON WSO AP	42.22	75.98
MAINE				300785	BOONVILLE 3 SE	43.45	75.32
170275	AUGUSTA FAA ARPT	44.32	69.80	300889	BRIDGEHAMPTON	40.95	72.30
170355	BANGOR FAA AIRPORT	44.80	68.82	301012	BUFFALO WSCMO AP	42.93	78.73
171175	CARIBOU WSO AIRPORT	46.87	68.02	301185	CANTON	44.58	75.13
171628	CORINNA	44.93	69.26	301387	CHASM FALLS	44.75	74.22
172426	EASTPORT	44.92	67.00	301623	COLDEN 1 N	42.67	78.68
172878	FORT KENT	47.25	68.59	301752	COOPERSTOWN	42.70	74.92
173892	HOULTON FAA AIRPORT	46.13	67.79	301799	CORTLAND	42.60	76.18
176905	PORTLAND WSMO ARPT	43.65	70.32	301974	DANSVILLE	42.57	77.71
176937	PRESQUE ISLE	46.65	68.00	302129	DOBBS FERRY	41.02	73.87
177325	RUMFORD 3 SW	44.53	70.54	302554	ELIZABETHTOWN 1 N	44.22	73.59
178398	SQUA PAN DAM	46.55	68.33	302610	ELMIRA	42.09	76.80
MARYLAND				303025	FRANKLINVILLE	42.33	78.46
180465	BALTIMORE WSO AIRPORT	39.22	76.60	303033	FREDONIA	42.44	79.34
180732	BENSON POLICE BARRACKS	39.50	76.38	303259	GLENHAM	41.52	73.93
181385	CAMBRIDGE 5 W	38.57	76.11	303284	GLENS FALLS FARM	43.33	73.73
181750	CHESTERTOWN	39.22	76.07	303294	GLENS FALLS FAA AIRPORT	43.35	73.62
181995	COLLEGE PARK	38.98	76.94	303319	GLOVERSVILLE	43.05	74.34
182906	EMMITTSBURG 2 SE	39.68	77.30	303346	GOUVERNEUR	44.34	75.50
183675	GLENN DALE BELL STN	39.65	77.73	303360	GRAFTON 2 N	42.78	73.46
183975	HAGERSTOWN	39.70	78.18	304174	ITHACA CORNELL UNIV	42.45	76.46
184030	HANCOCK FRUIT LAB	38.53	76.99	304647	LAWRENCEVILLE	44.75	74.66
185080	LA PLATA	39.26	75.85	304731	LIBERTY	41.80	74.74
185985	MILLINGTON	39.40	79.40	304791	LITTLE FALLS CITY RSVR	43.07	74.87
186620	OAKLAND 1 SE	38.72	76.18	304808	LITTLE VALLEY	42.25	78.81
187806	ROYAL OAK 2 SSW	38.37	75.58	304844	LOCKPORT 2 NE	43.18	78.65
188000	SALISBURY	38.33	75.52	304849	LOCKPORT 4 NE	43.20	78.63
188005	SALISBURY FAA ARPT	39.51	79.13	305134	MASSENA FAA AIRPORT	44.93	74.85
188065	SAVAGE RIVER DAM	38.20	75.39	305377	MINEOLA	40.73	73.63
188380	SNOW HILL	39.33	76.87	305426	MOHONK LAKE	41.77	74.15
189750	WOODSTOCK			305597	MOUNT MORRIS 2 W	42.73	77.90
MASSACHUSETTS				305796	NEW YORK BENSONHURST	40.60	73.98
190120	AMHERST	42.39	72.53	305801	NEW YORK CENTRAL PARK	40.78	73.97
190535	BEDFORD	42.47	71.28	305811	NEW YORK LAGUARDIA WSO	40.77	73.89
190666	BIRCH HILL DAM	42.63	72.12	305821	NEW YORK WESTERLEIGH	40.60	74.17
190736	BLUE HILL	42.22	71.12	306085	NORWICH	42.53	75.52
190770	BOSTON ARPT	42.37	71.03	306314	OSWEGO EAST	43.47	76.51
192107	EAST BRIMFIELD DAM	42.12	72.13	306441	PATCHOGUE	40.78	73.03
192451	EAST WAREHAM	41.77	70.67	306659	PLATTSBURGH	44.66	73.47
193505	HAVERHILL	42.77	71.07	306774	PORT JERVIS	41.38	74.68
193624	HINGHAM	42.23	70.92	306820	POUGHKEEPSIE FAA ARPT	41.63	73.88
193985	KNIGHTVILLE DAM	42.28	72.87	307134	RIVERHEAD RESEARCH FARM	40.97	72.72
196783	READING	42.52	71.13	307167	ROCHESTER WSO AP	43.13	77.67
198573	TULLY DAM	42.63	72.22	307484	SARATOGA SPRINGS 7 SE	43.03	73.81
199316	WEST MEDWAY	42.13	71.43	307799	SLIDE MOUNTAIN	42.02	74.42
199923	WORCESTER WSO AIRPORT	42.27	71.87	307842	SODUS	43.21	77.04
NEW HAMPSHIRE				308088	SPENCER	42.22	76.51
270703	BETHLEHEM	44.28	71.69	308383	SYRACUSE WSO AIRPORT	43.11	76.16
270741	BLACKWATER DAM	43.32	71.72	308600	TROY LOCK AND DAM 2	42.75	73.68
271683	CONCORD WSO AIRPORT	43.20	71.51	308651	TUPPER LAKE SUNMOUNT	44.23	74.43
272174	DURHAM	43.14	70.94	308737	UTICA CAA	43.15	75.38
272999	FIRST CONNECTICUT LAKE	45.08	71.28	308936	WALTON	42.17	75.13
273850	HANOVER	43.70	72.28	308944	WANAKENA RANGER SCHOOL	44.15	74.90
274399	KEENE	42.92	72.27	309000	WATERTOWN	43.97	75.87
274656	LEBANON FAA AIRPORT	43.63	72.32	309005	WATERTOWN FAA AIRPORT	44.00	76.02
276697	PETERBORO 2 S	42.85	71.95	309189	WESTFIELD	42.28	79.60
276818	PINKHAM NOTCH	44.27	71.25	309292	WEST POINT	41.38	73.97
278539	SURRY MOUNTAIN DAM	43.00	72.32	OHIO			
NEW JERSEY				331072	BUCYRUS SEWAGE PLANT	40.81	82.97
280311	ATLANTIC CITY WSO AP	39.45	74.57	331458	CHARDON	41.58	81.19
280346	AUDUBON	39.88	75.08	331541	CHIPPEWA LAKE WATER WOR	41.06	81.92
281335	CANOE BROOK	40.75	74.35	331657	CLEVELAND WSO AIRPORT	41.42	81.87
281582	CHARLOTTEBURG	41.03	74.43	331786	COLUMBUS WSO AIRPORT	39.99	82.88
283029	FLEMINGTON 1 NE	40.54	74.86	331890	COSHOCOTON 2 N	40.26	81.87
283951	HIGHTSTOWN 1 N	40.28	74.54	332119	DELAWARE	40.28	83.07
284229	INDIAN MILLS 2 W	39.80	74.78	332251	DORSET 2 E	41.68	80.65
284635	LAMBERTVILLE	40.37	74.95	332599	ELYRIA 3 E	41.38	82.05
284987	LONG BRANCH	40.29	74.00	332786	FINDLAY FAA AIRPORT	41.02	83.67
285581	MILLVILLE FAA AIRPORT	39.37	75.07	332791	FINDLAY SEWAGE PLANT	41.05	83.67
286026	NEWARK WSO AIRPORT	40.70	74.17	333758	HILLSBORO 1 E	39.18	83.61
				333780	HIRAM	41.31	81.15
				333874	HOYTVILLE 2 NE	41.22	83.77
				333987	IRWIN	40.12	83.48
				334865	MANSFIELD WSO AIRPORT	40.82	82.52
				334942	MARION WATER WORKS	40.61	83.14

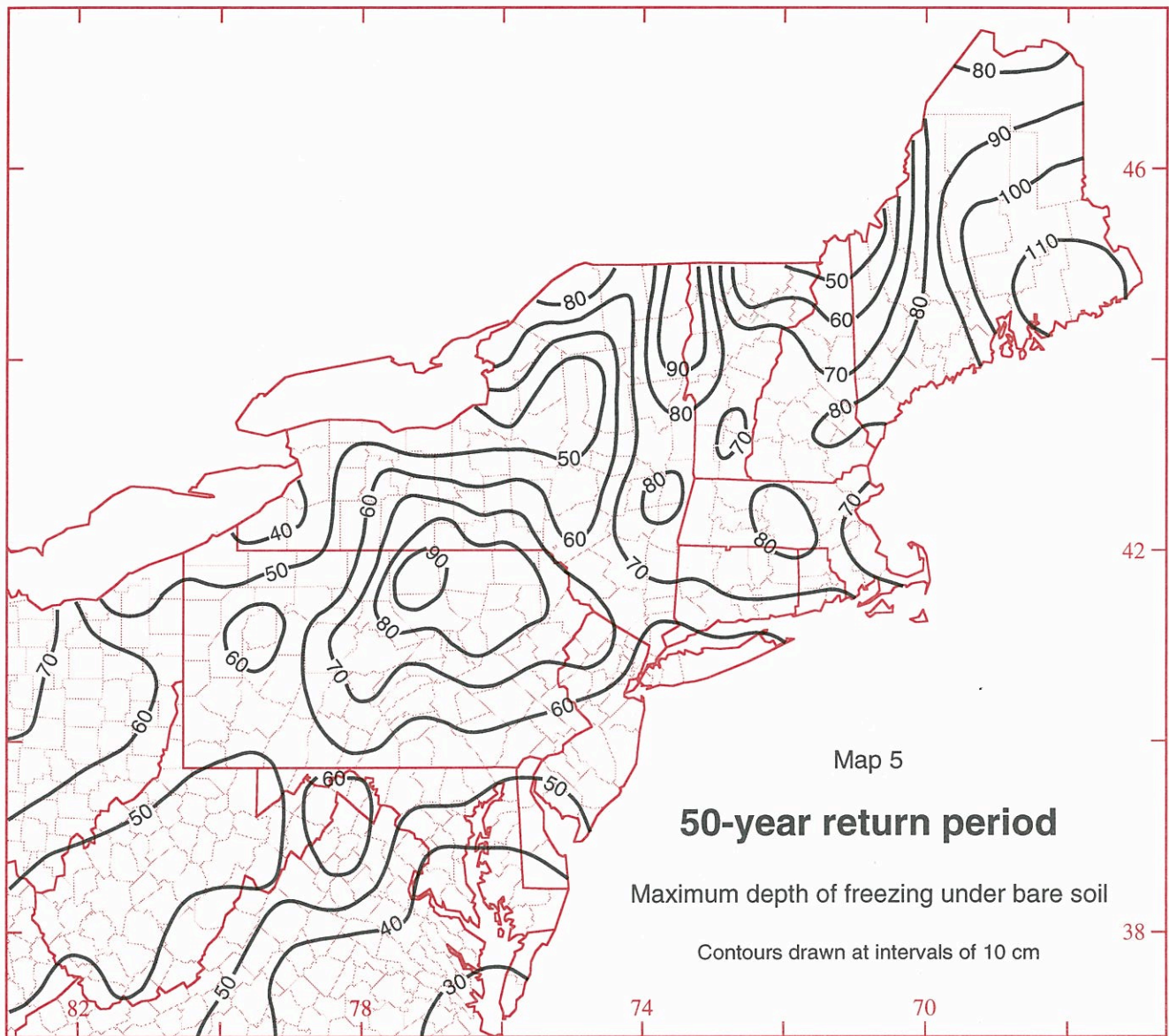
Station #	Station name	Latitude (degrees)	Longitude (degrees)	Station #	Station name	Latitude (degrees)	Longitude (degrees)
OHIO (continued)				VIRGINIA (continued)			
334979	MARYSVILLE	40.23	83.37	442208	DALE ENTERPRISE	38.45	78.93
335041	MC CONNELSVILLE LOCK	39.65	81.85	442941	FARMVILLE	37.32	78.38
335356	MINERAL RIDGE WTR WKS	41.15	80.78	444128	HOT SPRINGS	38.00	79.83
335747	NEWARK WATER WORKS	40.08	82.42	444720	LANGLEY AIR FORCE BASE	37.08	76.35
335857	NEW LEXINGTON 2 NW	39.73	82.22	444876	LEXINGTON	37.78	79.43
335894	NEW PHILADELPHIA	40.50	81.45	444909	LINCOLN	39.12	77.72
336118	NORWALK HIWAY DEPT	41.26	82.62	445050	LOUISA	38.03	78.00
336405	PANDORA 2 NE	40.97	83.96	445096	LURAY 5 E	38.67	78.38
336600	PHILO 3 SW	39.83	81.92	445120	LYNCHBURG WSO AIRPORT	37.33	79.20
336781	PORTSMOUTH	38.74	82.91	445851	MOUNT WEATHER	39.07	77.88
336882	PUT IN BAY STONE LAB	41.65	82.82	446475	PAINTER 2 W	37.58	75.82
337447	SANDUSKY	41.45	82.72	446712	PIEDMONT FIELD STN	38.22	78.11
338313	TIFFIN	41.12	83.17	447201	RICHMOND WSO AIRPORT	37.50	77.33
338357	TOLEDO EXPRESS WSO AP	41.60	83.80	447285	ROANOKE WSO AIRPORT	37.32	79.97
338534	UPPER SANDUSKY	40.83	83.28	447338	ROCKY MOUNT	37.00	79.90
338769	WARREN	41.22	80.83	448448	TIMBERVILLE 2 N	38.65	78.74
338794	WASHINGTON COURT HOUSE	39.52	83.42	448829	WALKERTON	37.74	77.04
338951	WESTERVILLE	40.13	82.94	448888	WARRENTON 5 NE	38.72	77.75
339219	WILMINGTON	39.48	83.83	448894	WARSAW 2 N	37.98	76.77
339312	WOOSTER EXP STN	40.78	81.93	448906	WASHINGTON NATL WSO AP	38.85	77.03
339406	YOUNGSTOWN WSO AIRPORT	41.25	80.67	449025	WEST POINT 2 SW	37.52	76.82
339417	ZANESVILLE FAA AIRPORT	39.95	81.90	449151	WILLIAMSBURG	37.29	76.70
				449186	WINCHESTER RESEARCH LAB	39.18	78.15
				449263	WOODSTOCK	38.89	78.49
PENNSYLVANIA				WEST VIRGINIA			
360106	ALLEN TOWN WSO AIRPORT	40.65	75.43	460527	BAYARD	39.27	79.37
360865	BRADFORD FAA AIRPORT	41.80	78.63	460580	BECKLEY VA HOSPITAL	37.78	81.18
360868	BRADFORD 4 W RES 1	41.93	78.73	460921	BLUEFIELD FAA AP	37.30	81.22
361354	CHAMBERSBURG	39.93	77.63	460939	BLUESTONE DAM	37.64	80.88
361485	CLARION 3 SW	41.20	79.43	461220	BUCKHANNON 2 W	39.00	80.26
361705	CONFLUENCE 1 SW DAM	39.80	79.37	461393	CANAAN VALLEY	39.05	79.43
361790	CORRY	41.92	79.63	461570	CHARLESTON WSO AIRPORT	38.37	81.60
362260	DUBOIS FAA AP	41.18	78.90	461677	CLARKSBURG 1	39.27	80.35
362682	ERIE WSO ARPT	42.08	80.18	462718	ELKINS WSO AIRPORT	38.69	79.85
362942	FORD CITY 4 S DAM	40.72	79.50	462920	FAIRMONT	39.47	80.14
363028	FRANKLIN	41.38	79.82	463072	FLAT TOP	37.58	81.10
363526	GREENVILLE	41.41	80.38	463353	GARY	37.37	81.55
363662	HANOVER	39.80	76.98	463544	GLENVILLE 1	38.94	80.82
363699	HARRISBURG WSO	40.22	76.85	463846	HAMLIN	38.28	82.10
363758	HAWLEY	41.48	75.17	464393	HUNTINGTON FAA AIRPORT	38.37	82.55
364214	INDIANA 3 SE	40.60	79.12	465563	MADISON	38.05	81.82
364325	JAMESTOWN 2 NW	41.50	80.47	465707	MARTINSBURG MUNICIPAL AP	39.40	77.98
364432	KANE 1 NNE	41.68	78.80	465739	MATHIAS	38.87	78.87
364778	LANDISVILLE	40.11	76.43	465963	MIDDLEBOURNE 2 ESE	39.48	80.87
365336	MADERA	40.82	78.42	466202	MORGANTOWN MUNICIPAL AP	39.65	79.92
365408	MARION CENTER 2 SE	40.75	79.03	466591	OAK HILL	37.97	81.15
365606	MEADVILLE 1 S	41.63	80.17	466849	PARKERSBURG FAA AP	39.35	81.43
365817	MILLVILLE 2 SW	41.10	76.57	466859	PARKERSBURG WSO	39.27	81.55
365902	MONTGOMERY DAM	40.65	80.38	466867	PARSONS	39.10	79.67
365915	MONTROSE 3 E HIWAY SHED	41.83	75.85	467029	PINEVILLE 1 NE	37.58	81.53
366297	NEWPORT	40.48	77.13	467552	RIPLEY	38.87	81.68
366889	PHILADELPHIA WSO AP	39.88	75.24	467730	ROMNEY	39.35	78.76
366916	PHILIPSBURG FAA AIRPORT	40.91	78.07	467785	ROWLESBURG 1	39.34	79.68
366993	PITTSBURGH WSCMO 2 AP	40.50	80.22	469011	UNION	37.57	80.53
367029	PLEASANT MOUNT 1 W	41.73	75.45	469281	WARDENSVILLE RM FARM	39.10	78.58
367229	PUTNEYVILLE 2 SE DAM	40.93	79.28	469436	WESTON	39.06	80.47
367477	RIDGWAY	41.42	78.75	469683	WINFIELD LOCKS	38.53	81.92
367782	SALINA 3 W	40.52	79.55				
368073	SHIPPENSBURG	40.05	77.52				
368184	SLIPPERY ROCK	41.06	80.06				
368449	STATE COLLEGE	40.80	77.87				
368596	STROUDSBURG 2 E	40.99	75.19				
368873	TIONESTA 2 SE DAM	41.48	79.43				
368905	TOWANDA	41.76	76.43				
369298	WARREN 1 SSW	41.84	79.15				
369367	WAYNESBURG 1 E	39.90	80.17				
369408	WELLSBORO 3 S	41.71	77.27				
369728	WILLIAMSPORT 4E WSO AP	41.25	76.92				
369933	YORK 3 SSW PUMP STN	39.92	76.75				
RHODE ISLAND							
374266	KINGSTON	41.48	71.53				
376698	PROVIDENCE WSO AIRPORT	41.73	71.43				
VERMONT							
430499	BELLOWS FALLS	43.13	72.45				
431081	BURLINGTON WSO AP	44.47	73.15				
431243	CAVENDISH	43.38	72.60				
431360	CHELSEA 2 S	43.98	72.46				
435278	MONTPELIER FAA AIRPORT	44.20	72.57				
435416	MOUNT MANSFIELD	44.53	72.82				
435542	NEWPORT	44.93	72.20				
436761	READSBORO 1 SSE	42.75	72.93				
436995	RUTLAND	43.61	72.97				
437054	ST JOHNSBURY	44.42	72.02				
438600	VERNON	42.77	72.52				
VIRGINIA							
440720	BIG MEADOWS 2	38.52	78.43				
440766	BLACKSBURG 2	37.21	80.42				
441209	BURKES GARDEN	37.09	81.33				
441593	CHARLOTTESVILLE 2 W	38.03	78.52				
442009	CORBIN	38.20	77.37				

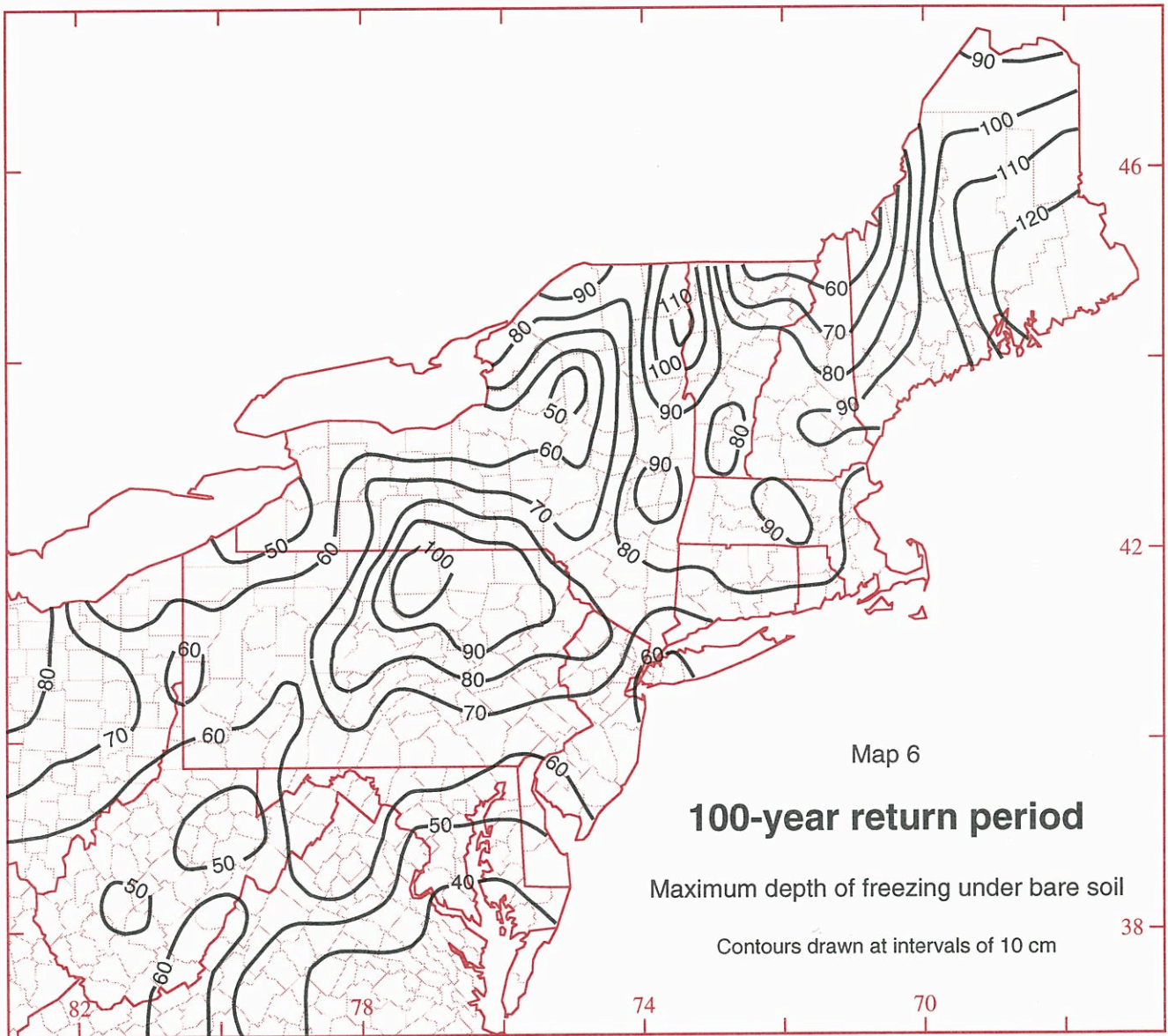


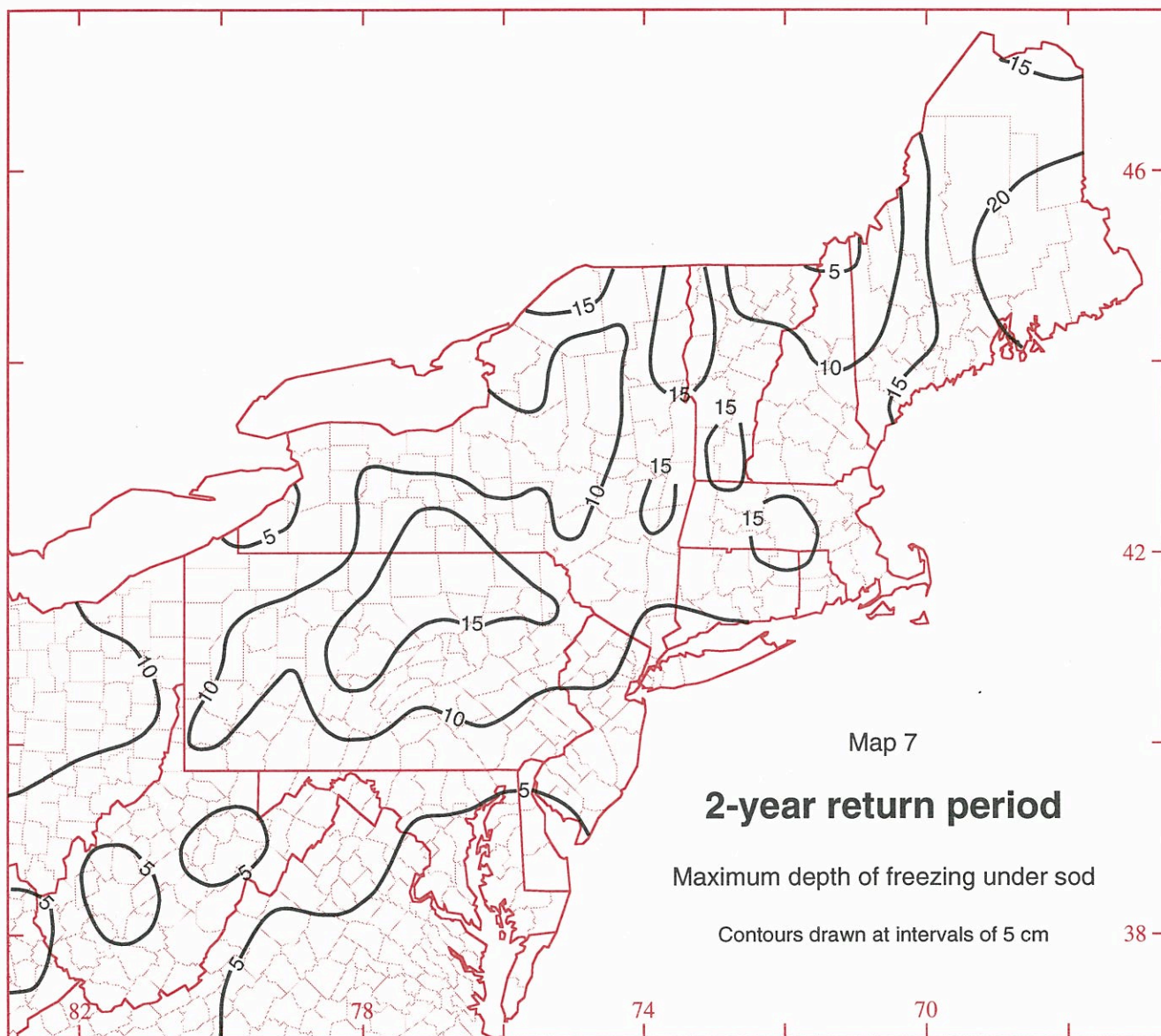


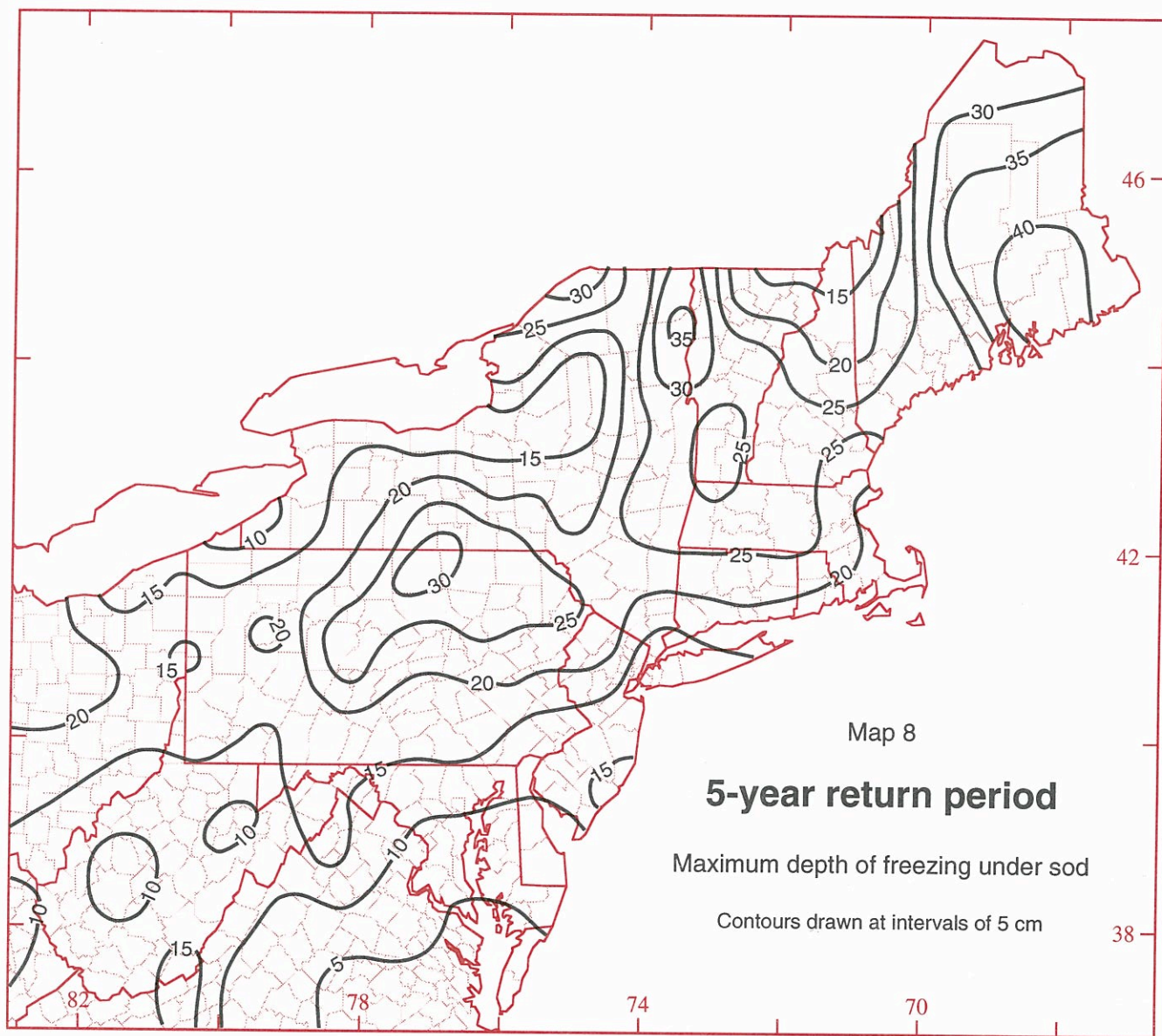


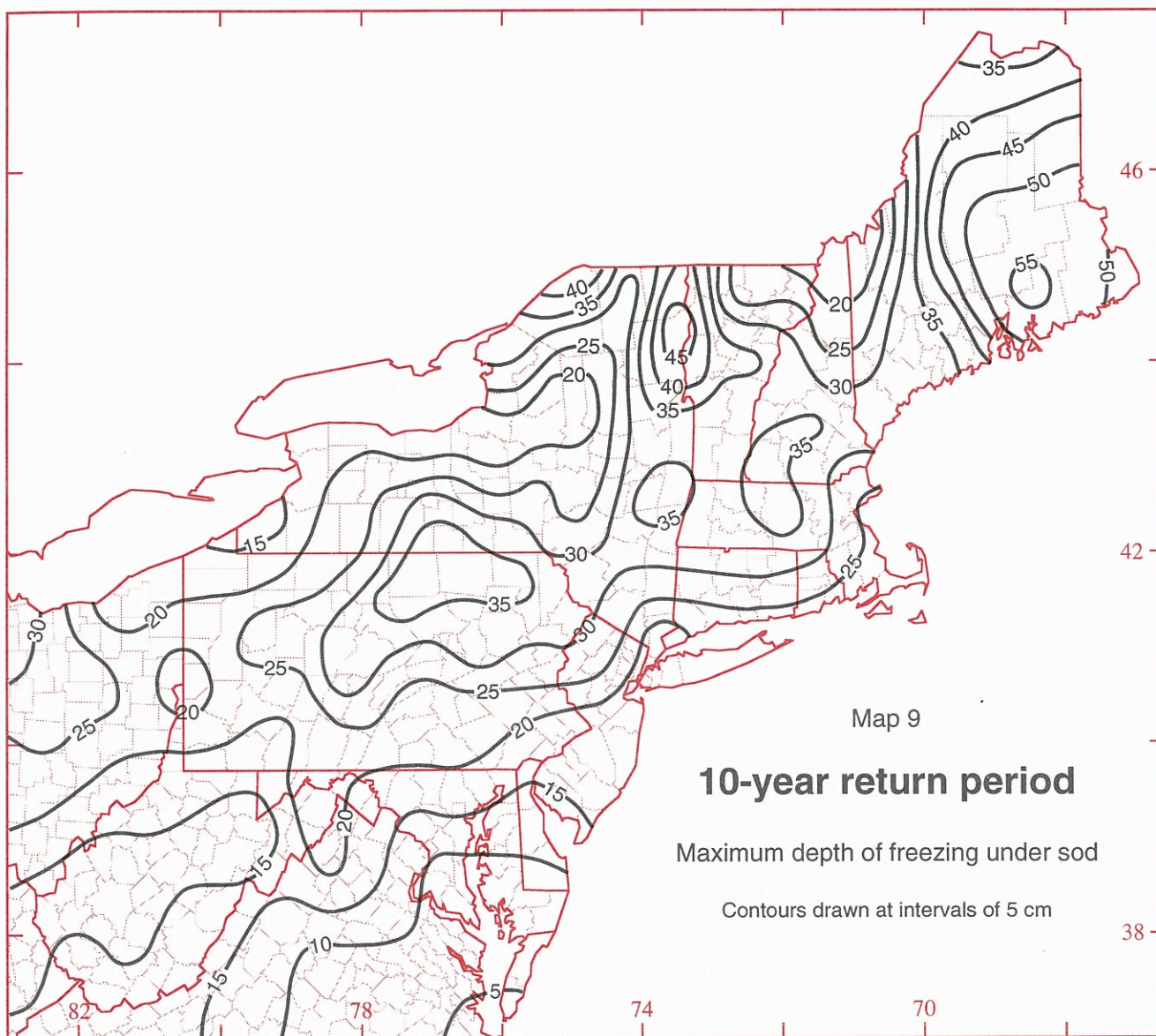


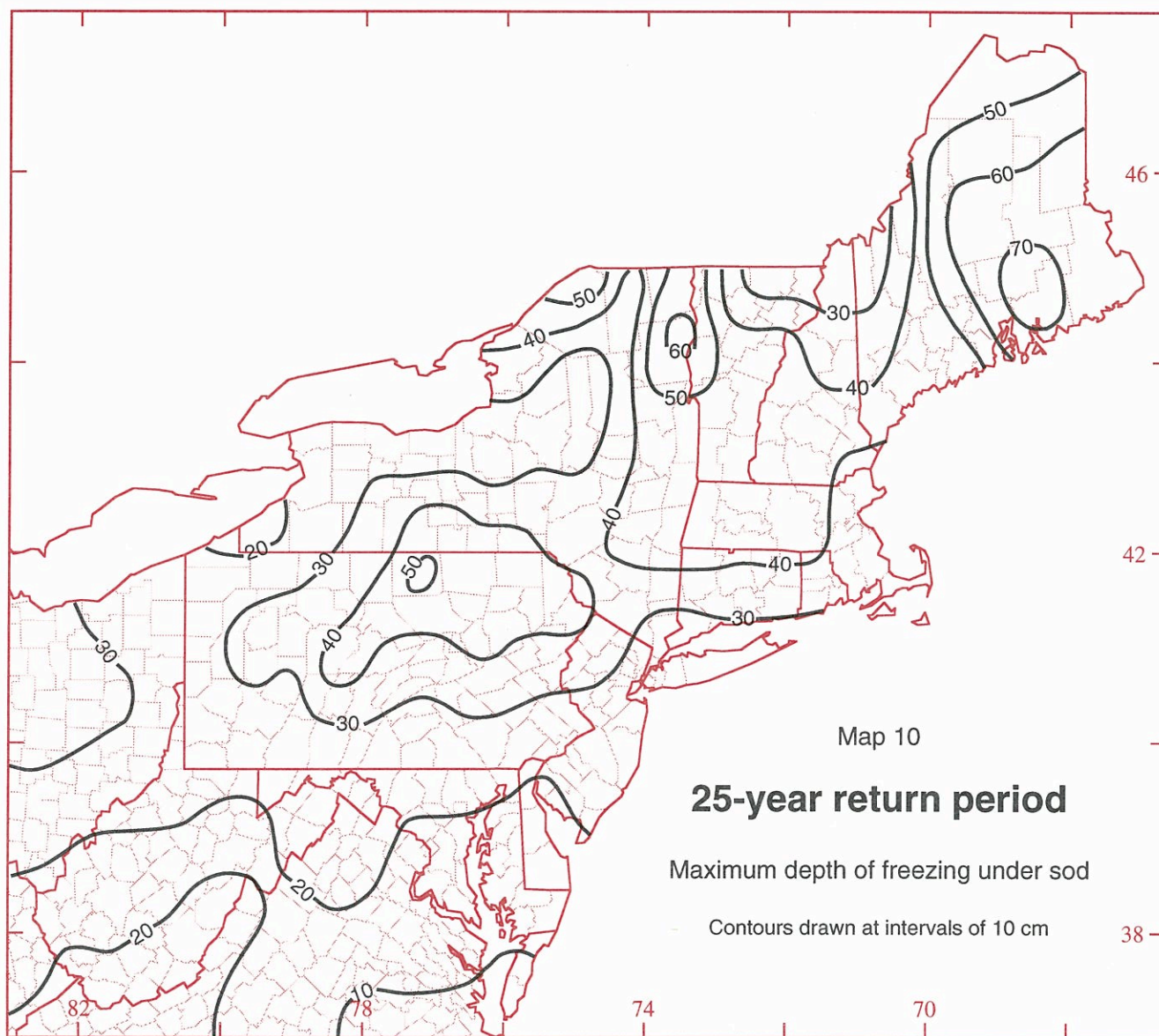


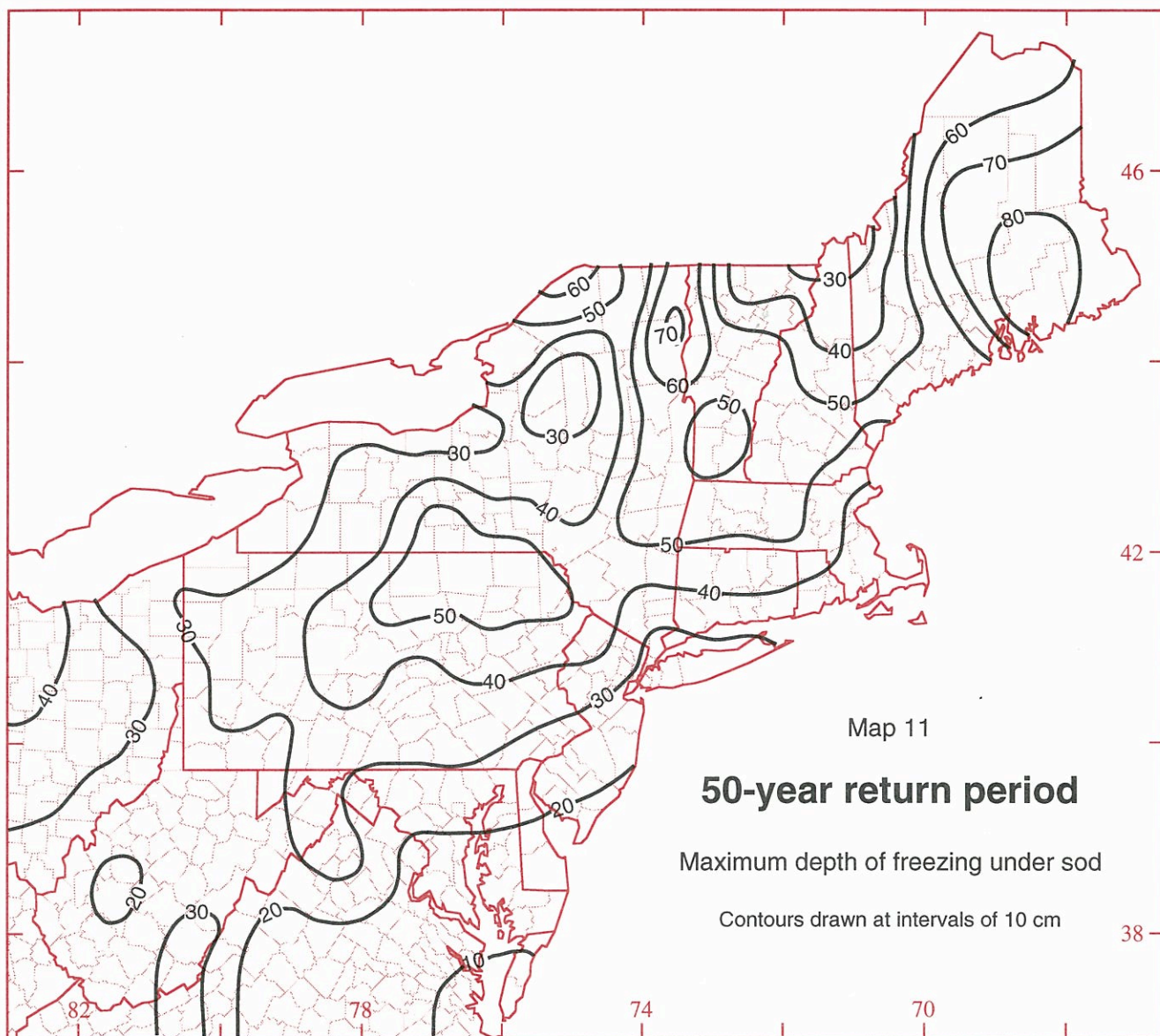


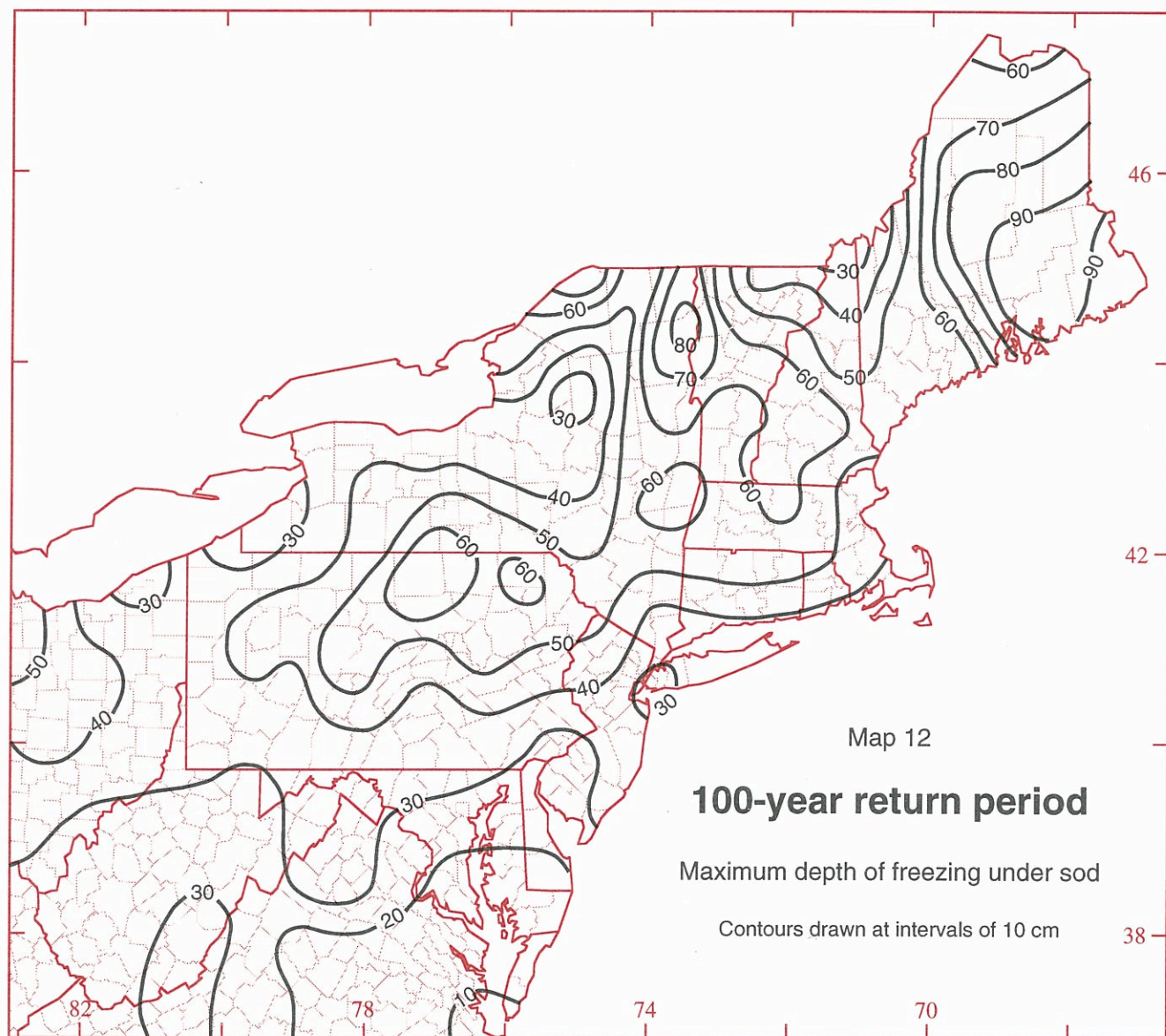


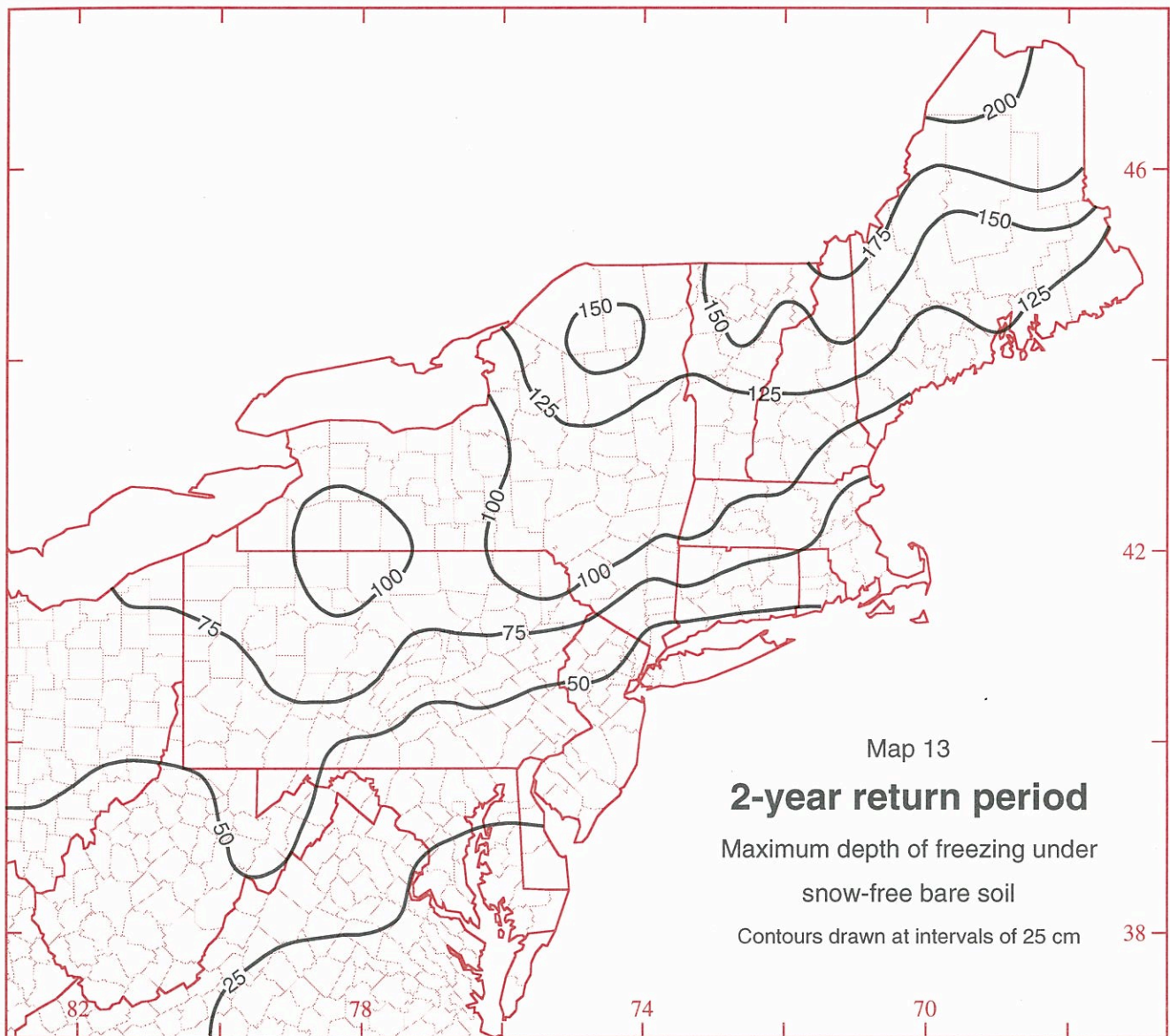


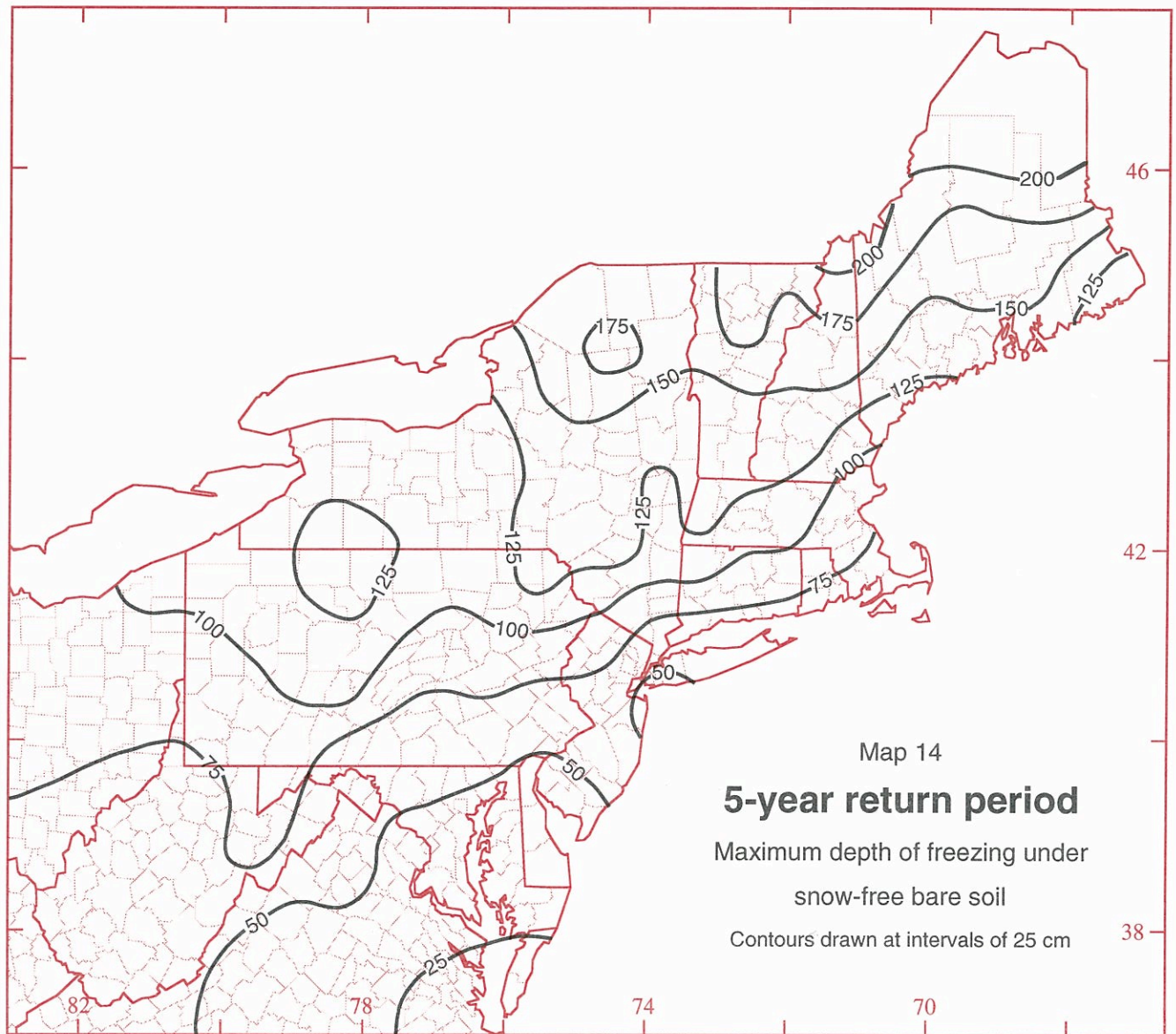


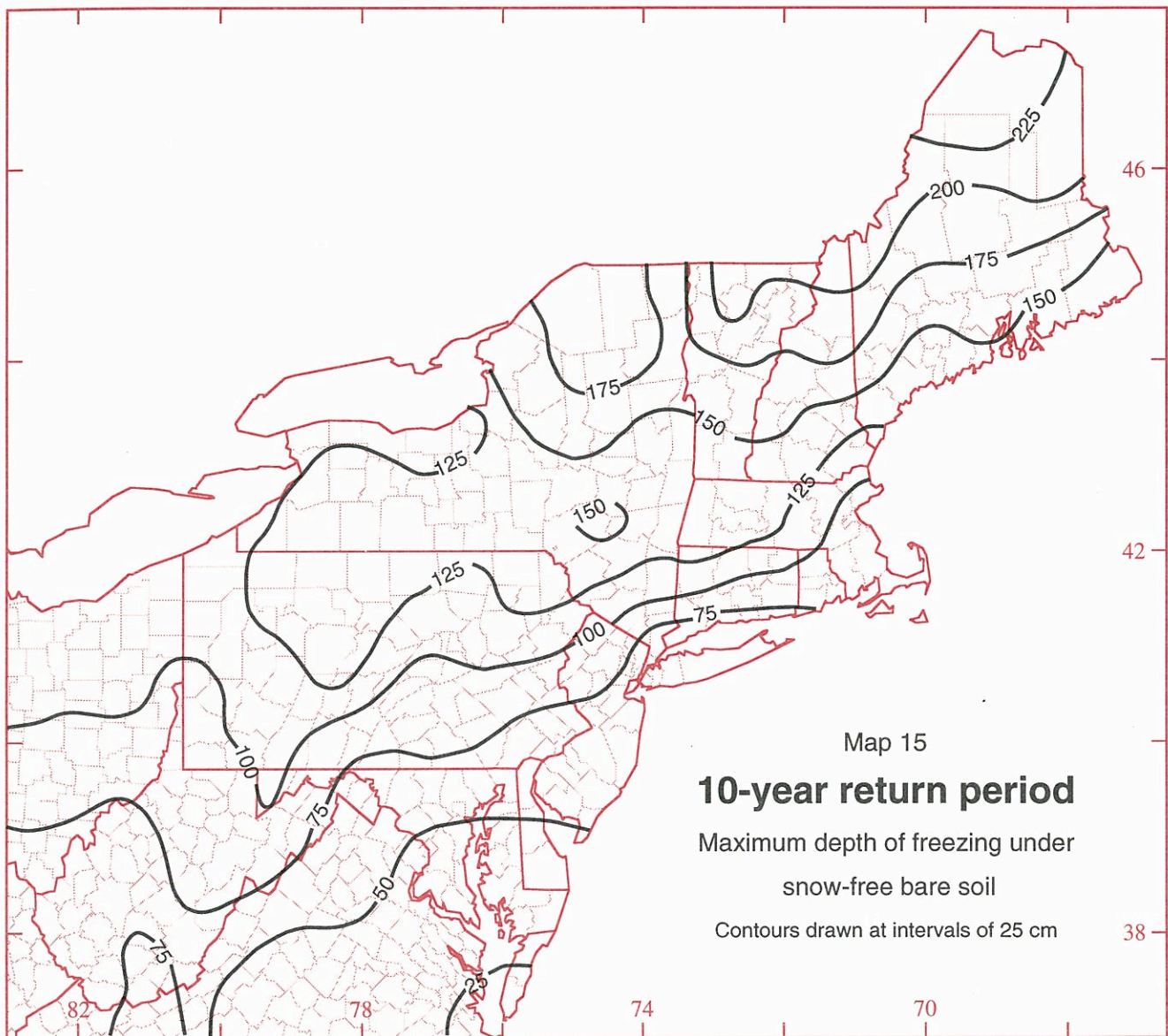


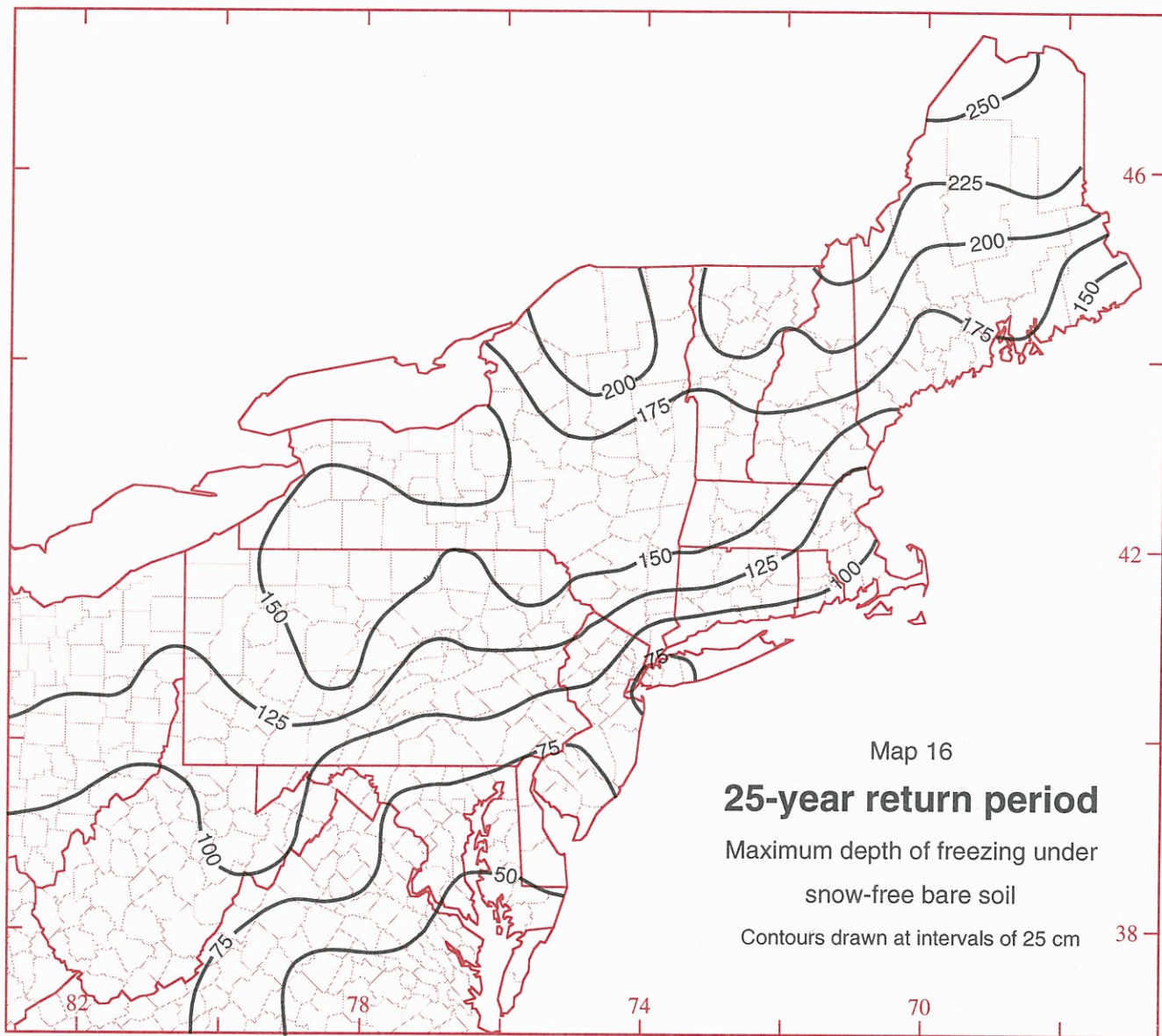


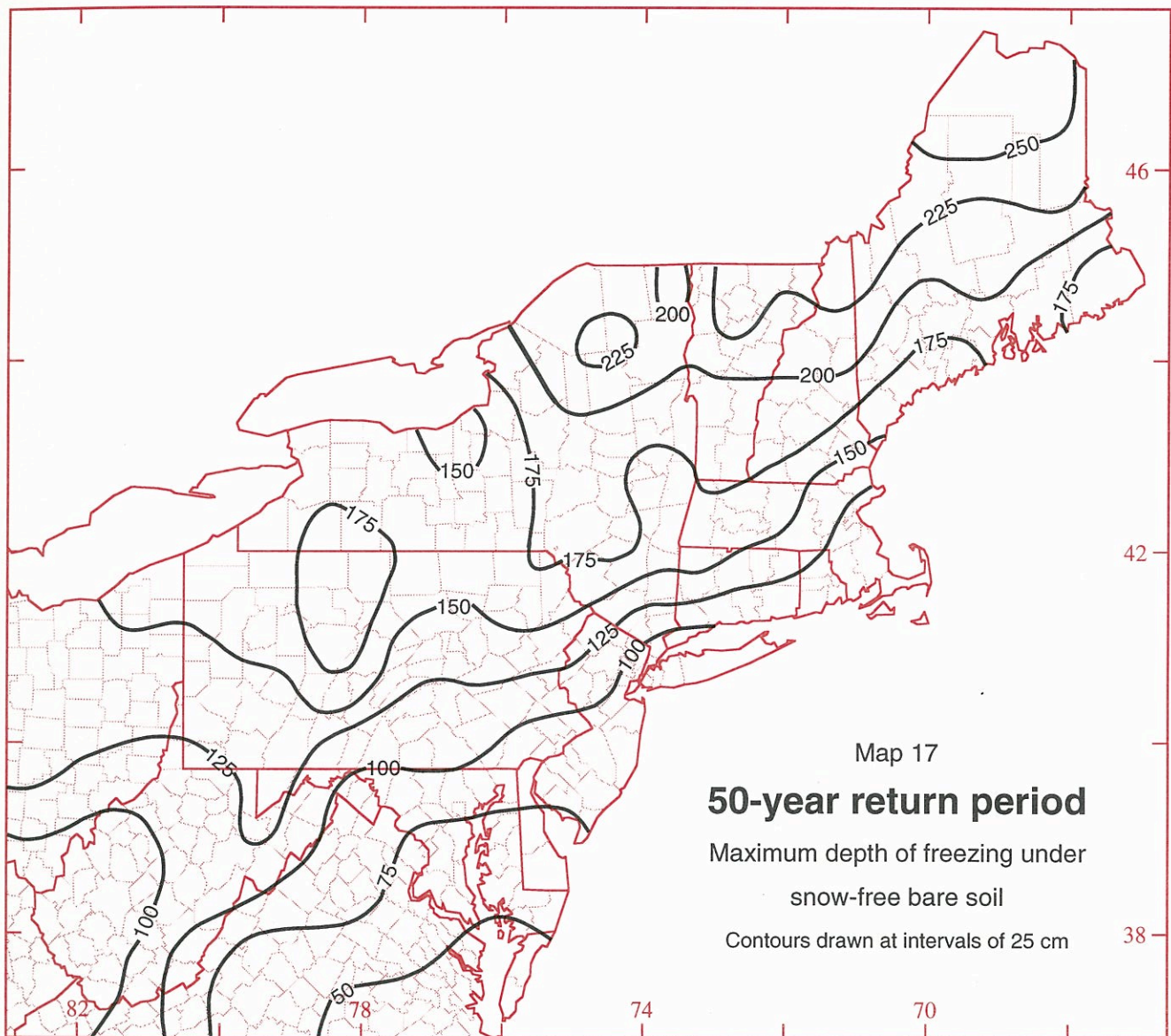


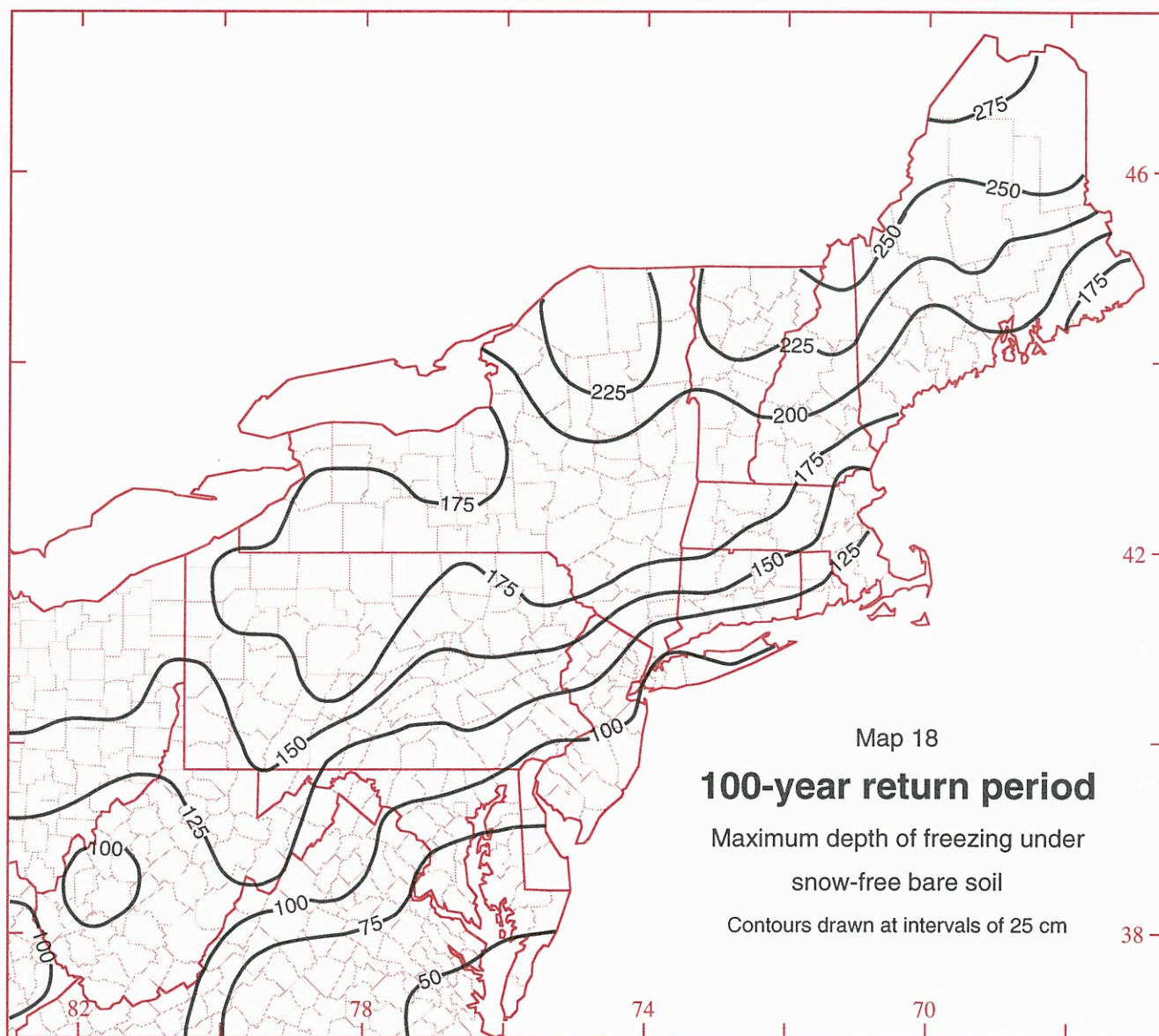












RECENT NRCC RESEARCH SERIES PUBLICATIONS

- Samelson, D., *A Simple Method for Predicting Snowpack Water Equivalent in the Northeastern United States*, NRCC Research Publication RR 92-1.
- Wilks, D.S., *Spline Interpolated Parameters for Adjusting Climatological Precipitation Distributions using the 30- and 90-Day Outlooks*, NRCC Research Publication RR 92-2.
- Cember, R.P. and D.S. Wilks, *Climatological Atlas of Snowfall and Snow Depth for the Northeastern United States and Southeastern Canada*, NRCC Research Publication RR 93-1.
- DeGaetano, A.T., K.L. Eggleston, and W.W. Knapp, *A Method to Produce Serially Complete Daily Maximum and Minimum Temperature Data for the Northeast*, NRCC Research Publication RR 93-2.
- DeGaetano, A.T., W.W. Knapp, and K.L. Eggleston, *Standardizing Growing Degree Day Totals for Differences in Temperature Observing Schedules*, NRCC Research Publication RR 93-3.
- DeGaetano, A.T., K.L. Eggleston, and W.W. Knapp, *Daily Solar Radiation Estimates for the Northeastern United States*, NRCC Research Publication RR 93-4.
- Wilks, D.S. and R.P. Cember, *Atlas of Precipitation Extremes for the Northeastern United States and Southeastern Canada*, NRCC Research Publication RR 93-5.
- DeGaetano, A.T., K.L. Eggleston, and W.W. Knapp, *Climatology of Extreme Maximum Temperature Occurrences for the Northeastern United States*, NRCC Research Publication RR 93-6.
- DeGaetano, A.T., K.L. Eggleston, and W.W. Knapp, *Daily Evapotranspiration and Soil Moisture Estimates for the Northeastern United States*, NRCC Research Publication RR 94-1.
- Leathers, D.J., *A Tornado Climatology for the Northeastern United States*, NRCC Research Publication RR 94-2.
- Wilks, D.S., and M. McKay, *Atlas of Extreme Snow Water-Equivalent for the Northeastern United States*, NRCC Research Publication RR 94-3.
- McKay, M., and D.S. Wilks, *Atlas of Short-Duration Precipitation Extremes for the Northeastern United States and Southeastern Canada*, NRCC Research Publication RR 95-1.
- DeGaetano, A.T., K.L. Eggleston, and W.W. Knapp, *Atlas of Growing Degree Day Statistics for the Northeastern United States and Southeastern Canada*, NRCC Research Publication RR 95-2.

NRCC DIGITAL DATA SETS

- Eggleston, K.L. and D.S. Wilks, *Gridded Monthly Precipitation Distribution Parameters for the Continental United States*, NRCC Data Set DS 92-1.
- Cember, R.P., K.L. Eggleston, and D.S. Wilks, *Digital Snowfall and Snow Depth Probabilities for the Northeastern United States and Southeastern Canada*, NRCC Data Set DS 93-1.
- McKay, M., D.S. Wilks, and T.W. Schmidlin, *Quality-Controlled Snow Water Equivalent Data for the Northeastern United States*, NRCC Data Set DS 94-1.

CORNELL
UNIVERSITY

Department of Soil, Crop and Atmospheric Sciences
Ithaca, New York 14853